Unique microbial catabolic pathway for the human-core *N*-glycan constituent fucosyl-α-1,6-*N*-acetylglucosamine-asparagine

Running title: Glycoamino acid catabolism by *Lactobacillus casei*

Jimmy E. Becerra,[a] Jesús Rodríguez-Díaz,[b] Roberto Gozalbo-Rovira,[b] Martina Palomino-Schätzlein,[c] Manuel Zúñiga,[a] Vicente Monedero,[a] María J. Yebra[a]#

[a]Laboratorio de Bacterias Lácticas y Probióticos, Departamento de Biotecnología de Alimentos, IATA-CSIC, Paterna, Spain.

[b]Departamento de Microbiología, Facultad de Medicina, Universidad de Valencia, Valencia, Spain.

[c]NMR facility, Centro de Investigación Príncipe Felipe, Valencia, Spain.

#Address correspondence to María J. Yebra, yebra@iata.csic.es

Number of words in the abstract: 249

Number of words in the text: 5856

ABSTRACT

The survival of commensal bacteria in the human gut partially depends on their ability to metabolize host-derived molecules. The use of the glycosidic moiety of *N*-glycoproteins by bacteria has been reported, but the role of *N*-glycopeptides or glycoamino acids as substrates for bacterial growth has not been evaluated. We have identified in *Lactobacillus casei* strain BL23 a gene cluster (*alf2*), involved in the catabolism of the glycoamino acid fucosyl-α-1,6-*N*-GlcNAc-Asn (6'FN-Asn), a constituent of the core-fucosylated structures of mammalian *N*-glycoproteins. The cluster consists of the genes *alfHC*, encoding a MFS permease and the α-L-fucosidase AlfC, and the divergently oriented *asdA* (aspartate 4-decarboxylase), *alfR2* (transcriptional regulator), *pepV* (peptidase), *asnA2* (glycosyl-asparaginase) and *sugK* (sugar kinase) genes. Knockout mutants showed that *alfH, alfC*, *asdA*, *asnA2* and *sugK* are necessary for efficient 6'FN-Asn utilization. The *alf2* genes are induced by 6'FN-Asn, but not by its glycan moiety, via the AlfR2 regulator. Constitutive expression of *alf2* genes in an *alfR2* strain allowed metabolism of a variety of 6'fucosyl-glycans. However, GlcNAc-Asn did not support growth in this mutant background, indicating that the presence of a 6´fucose moiety is crucial for substrate transport via AlfH. Within the bacteria, 6'FN-Asn is defucosylated by AlfC generating GlcNAc-Asn. This glycoamino acid is processed by the glycosylasparaginase AsnA2. GlcNAc-Asn hydrolysis generates aspartate and GlcNAc, which is used as a fermentable source by *L. casei.* These data establish the existence in a commensal bacterial species of an exclusive metabolic pathway likely to scavenge human milk and mucosal fucosylated-*N*-glycopeptides in the gastrointestinal tract.

IMPORTANCE

The gastrointestinal tract accommodates more than 10^{14} microorganisms that have an enormous impact in human health. The mechanisms enabling commensal bacteria and administered probiotics to colonize the gut remain largely unknown. The ability to utilize host-derived carbon and energy resources available at the mucosal surfaces may provide these bacteria with a competitive advantage in the gut. Here we have identified in the commensal species *Lactobacillus casei* a novel metabolic pathway for the utilization of the glycoamino acid fucosyl-α-1,6-*N*-GlcNAc-Asn, which is present at the core-fucosylated *N*-glycoproteins from mammalians. These results give insight into the molecular interactions between the host and the commensal/probiotics bacteria and may help to devise new strategies to restore gut microbiota homeostasis in diseases associated to dysbiotic microbiota.

INTRODUCTION

Many investigations have recently highlighted the importance of the gut microbiota in the onset and progression of a number of human diseases, including gastrointestinal disorders (1, 2), inflammatory diseases (3), respiratory tract infections (4) and allergies (5). The functional impact of commensal gut microorganisms depends on their ability to survive in the gastrointestinal tract, to adhere to epithelial mucus, and to obtain energy from non-digestible dietary substrates and host mucosal secretions (6). More than half of all proteins in nature have been estimated to be glycosylated through *O*-glycosidic or *N*-glycosidic bonds (7). *O*-glycans are linked to a serine or threonine residue via an *N*-acetylgalactosamine which is elongated by additional sugars (8). *N*-glycosylation is a common modification of extracellular membrane proteins present at the gastrointestinal epithelium, the secreted proteins of human breast milk and many dietary proteins (7, 9-11). *N*-linked glycans are attached via the core *N,N'*-diacetylchitobiose disaccharide (ChbNAc; GlcNAc-β1,4-GlcNAc) to an asparagine residue of proteins containing the Asn-Xxx-Ser/Thr (being Xxx any amino acid excepting Pro) motif (12). In *N*-glycans from mammalians, the inner GlcNAc moiety bound to Asn is often fucosylated through an α1,6-linkage, named as core fucose. Protein *N*-glycosylation plays a crucial role in a variety of cellular processes, such as cell adhesion (13), immune pathway signaling (14) and bacterial recognition (15). Some intestinal microorganisms have the ability to process the carbohydrate moieties of *N*-glycosylated proteins (16) so that the type, abundance and location of these glycans contribute to shape the composition and distribution of the gut microbiota (17). Some bacterial pathogens possess endo-β-*N*-acetylglucosaminidase enzymes that cleave the β-1,4-linkage of the core ChbNAc present in all *N*-glycoproteins, releasing the *N*-glycan moiety (18). The activity of these enzymes have been associated with the modification of the biological function of host defense glycoproteins such as immunoglobulins and lactoferrin (19-21), and with the use of the glycans as nutrients (21), for which they are considered virulence factors

(22). In commensal bacteria, the ability to remove *N*-glycans from glycoproteins has been described in a few *Bifidobacterium* species (23, 24). Recently, the importance of core-fucosylated *N*-glycans from human milk in promoting the intestinal growth of *Bifidobacterium* and *Lactobacillus* species has been demonstrated in lactating infants from mothers carrying different alleles of the fucosyltransferase Fut8, responsible for core fucosylation (25). This provides the first *in vivo* evidence of the importance of this core structure in feeding intestinal commensals. However, there is little information about the fate of the fucosyl-α-1,6-GlcNAc bound to proteins through the Asn residue (6'FN-Asn). This glycoamino acid possibly results from the combined action of endo-β-*N*-acetylglucosaminidase enzymes and proteases on *N*-glycosylated proteins (18, 23, 24). The amide bond between the amino acid and the GlcNAc residue is hydrolyzed by two different enzymes, peptide-*N*(4)-(β-*N*-acetylglucosaminyl)-L-asparaginases (Glycopeptide *N*-glycosidase; PNGase) (E.C. 3.5.1.52) and *N*(4)-(β-*N*-acetylglucosaminyl)-L-asparaginases (Glycosylasparaginase) (E.C. 3.5.1.26). Both types of enzymes are produced as precursors that undergo intramolecular autoproteolysis to produce the mature active proteins (26, 27), but, PNGases require the presence of more than two amino acid residues in the substrate (28), whereas glycosylasparaginases act only in asparagine-oligosaccharides containing one amino acid (29). Currently, bacterial PNGases have only been characterized from the human pathogens *Elizabethkingia meningoseptica* and *Elizabethkingia miricola* (30, 31), and from the soil bacterium *Terriglobus roseus* (32). In *E. meningoseptica*, a glycosylasparaginase has also been characterized (33, 34).

Lactobacillus casei is a lactic acid bacterium able to survive in the grastrointestinal tract (35, 36) that has been isolated from a wide variety of habitats, including breast-fed infant feces (37, 38), and several strains are commonly used as probiotics in functional foods (39, 40). Oligosaccharides present in human milk, such as lacto-*N*-biose and *N*-acetyllactosamine, and derived from mucins, as galacto-*N*-biose, can support the

108 growth of *L. casei* (41, 42). This species is also able to catabolize lacto-*N*-triose (43)
109 and fucosyl-α-1,3-*N*-acetylglucosamine (44), which are abundant carbohydrates that
110 form part of larger glycan structures from human gut mucosas and human milk. Unlike
111 glycans, catabolic pathways for *N*-glycopeptides in bacteria have not been described.
112 In this work, we have identified in *L. casei* BL23 a gene cluster, named *alf2*, involved in
113 the metabolism of the glycoamino acid fucosyl-α-1,6-*N*-GlcNAc-Asn (6'FN-Asn). The
114 results reported have enabled us to propose a catabolic pathway for 6'FN-Asn and α-
115 1,6-fucosylated *N*-glycans in bacteria.

RESULTS

Identification of the *L. casei alf2* gene cluster involved in the metabolism of the glycoamino acid 6'FN-Asn. We had previously shown that the disaccharide fucosyl-α-1,6-*N*-acetylglucosamine (6'FN) is hydrolyzed *in vitro* by the *L. casei* BL23 α-L-fucosidase AlfC (glycosyl hydrolase family 29, GH29) (45). However, this bacterium is unable to grow in the presence of 6'FN as a carbon source (44). Analysis of the DNA region (Accession Nº FM177140) (46) around *alfC* revealed a gene cluster named here as *alf2* (Fig. 1A). The cluster consists of genes *alfHC* (LCABL_RS14345 and LCABL_RS14350) which encode a Major Facilitator Superfamily (MFS) permease and AlfC, respectively, and, divergently oriented, genes *asdA* (LCABL_RS14340), *alfR2* (LCABL_RS14335), *pepV* (LCABL_RS14330), *asnA2* (LCABL_RS14325) and *sugK* (LCABL_RS14320). These genes encode proteins annotated as aspartate 4-decarboxylase (*asdA*), GntR family transcriptional regulator (*alfR2*), peptidase M20 (*pepV*), *N*(4)-(β-*N*-acetylglucosaminyl)-L-asparaginase (*asnA2*) and ROK (Repressor, ORF, Kinase) family protein (*sugK*). Two putative *rho*-independent terminators were identified, downstream *alfC* (Δ*G*, -13.5 kcal/mol) and *sugK* (Δ*G*, -17.0 kcal/mol). The high specificity of the α-L-fucosidase AlfC from *L. casei* BL23 for α1,6-linkages as those present at fucosyl-oligosaccharides (45, 47), together with the sequence analysis of the *alf2* cluster, particularly the presence of a gene coding for a hypothetical *N*(4)-(β-*N*-acetylglucosaminyl)-L-asparaginase, suggested that the *alf2* operon could be involved in the metabolism of the core 6'FN-Asn (Fig. 1). To test this hypothesis this glycoamino acid was synthesized by transfucosylation with the α-L-fucosidase AlfC. We had previously utilized AlfC in transglycosylation reactions with *p*-nitrophenyl-α-L-fucopyranoside as the donor and GlcNAc as the acceptor to produce 6'FN (47). Here, the ability of AlfC to use GlcNAc-Asn as the acceptor was tested and 6'FN-Asn was synthesized and purified. The purified 6'FN-Asn was characterized by nuclear magnetic resonance (NMR) spectroscopy (Fig. 2A) (See Fig. S1 and Table S1 in the

supplemental material). ChbNAc, galactose and glucose were also used in transfucosylation reactions with AlfC and the glycans fucosyl-α-1,6-*N,N'*-diacetylchitobiose (N2F *N*-glycan), which forms part of the core fucosylation, fucosyl-α-1,6-galactose (6'FucGal) and fucosyl-α-1,6-glucose (6'FucGlc) were also synthesized (Fig. 2B, C and D) (Table S1).

To determine whether *L. casei* BL23 is able to use 6'FN-Asn, GlcNAc-Asn, N2F *N*-glycan, 6'FucGal or 6'FucGlc as carbon sources, its growth profiles in MRS basal medium supplemented with each compound were analyzed. *L. casei* only grew in the presence of the glycoamino acid 6'FN-Asn (Fig. 3A). The analysis of the carbohydrate content of the growth media showed that BL23 did not degrade any of the assayed glycans (Fig. 3C). However, the AlfR2 deficient strain (BL405) could degrade all the synthesized 6'fucosyl oligosaccharides as evidenced by the quantitative accumulation of L-fucose in the supernatant and the disappearance of the peaks corresponding to the fucosylated substrates (Fig. 3C). The presence of L-fucose in the culture supernatants was due to the fact that *L. casei* does not metabolize L-fucose and excretes it to the culture medium (44). Nevertheless, growth with those carbon sources was very poor compared to 6'FN-Asn (Fig. 3B). Interestingly, like the wild-type, the *alfR2* mutant strain did not use GlcNAc-Asn (Fig. 3B). These results suggested that AlfR2 represses the expression of *alf2* genes and that the presence of 6'FN-Asn is required to relieve repression. Furthermore, the existence of an L-fucose moiety with α1,6 linkage configuration is possibly necessary for the uptake of the tested fucosyl oligosaccharides, including 6'FN-Asn.

Transcription of the *alf2* gene cluster is induced by 6'FN-Asn and repressed by AlfR2. To find out whether the transcription of the *alf2* genes is regulated by the glycoamino acid 6'FN-Asn or its glycan moiety, RT-qPCR experiments were performed with RNA isolated from *L. casei* BL23 grown with 6'FN-Asn, 6'FN, GlcNAc or glucose

(Fig. 4). The results showed that the *alf2* operon is induced by the glycoaminoacid 6'FN-Asn and not by the presence of 6'FN or GlcNAc, indicating that the glycoamino acid and not the glycan moiety is responsible for the induction of these genes and explaining the lack of growth of the wild type on N2F *N*-glycan, 6'FucGal and 6'FucGlc. In order to obtain direct evidence for the regulation of AlfR2 on these genes, RNA was isolated from the *alfR2* deletion strain BL405, cultured in the same conditions as the wild-type (Fig. 4). Regardless of the substrate tested, the expression of *alf2* genes was higher than in the wild-type growing on glucose, indicating that AlfR2 acts indeed as a transcriptional repressor.

The AlfC α-L-fucosidase and the AlfH permease are necessary for the metabolism of 6'FN-Asn and 6'fucosyl-oligosaccharides. To assess the role of *alfC* and *alfH* in the catabolism of 6'FN-Asn in *L. casei*, the growth patterns of mutant strains disrupted in *alfC* (BL415) and *alfH* (BL372) were analyzed in MRS basal medium supplemented with the fucosylated glycoamino acid (Fig. 5A and B). The profiles showed that both mutants failed to grow on 6'FN-Asn. To further confirm that the glycoamino acid was not fermented, culture supernatants analyses were performed and they showed that 6'FN-Asn remained in BL415 and BL372 supernatants without the appearance of L-fucose (Fig. 5E). The amount of L-fucose (1.12 mM) present in both supernatants corresponded to the L-fucose co-purified with the synthesized 6'FN-Asn (Fig. 2 and Fig. 5E). These results demonstrated that the α-L-fucosidase AlfC is involved in the metabolism of 6'FN-Asn and that the permease AlfH participates in its transport. To determine the role of AlfC and AlfH in the utilization of the rest of fucosyl-glycans synthesized here (6'FN, 6'FucGlc, 6'FucGal and N2F *N*-glycan) two double mutants strains, BL406 (*alfR2 alfC*) and BL407 (*alfR2 alfH*) were constructed. Both mutants showed growth patterns with 6'fucosyl-glycans similar to the negative control culture without added carbohydrate (Fig. 5C and D). In addition, the results showed a final culture O.D. of strains BL406 or BL407 significantly lower than strain BL405

198 (*alfR2*) on these sugars (Table S2). These results indicated that the α-L-fucosidase
199 AlfC and the permease AlfH are also involved in their metabolism and transport,
200 respectively. 6'FN-Asn was also tested as a carbon source in the culture medium with
201 these double mutants confirming the requirement of a functional α-L-fucosidase and
202 permease for its metabolism (Fig. 5C and D).
203
204 **6'FN-Asn catabolism requires AsdA, AsnA2 and SugK, but not PepV**. An *asdA*
205 mutant strain (BL416) showed an impaired growth in MRS basal medium
206 supplemented with 6'FN-Asn (Fig. 6A). Curiously, the glycoamino acid was completely
207 depleted from the culture supernatant (Fig. 5E); however the mutant strain reached a
208 lower optical density than the wild-type strain, suggesting that *asdA* is involved in 6'FN-
209 Asn metabolism. A BLAST search using the deduced amino acid sequence of AsdA
210 against the genomic sequence of *L. casei* BL23 did not reveal the presence of other
211 AsdA paralogues. AsdA belongs to the Asp aminotransferase family (cd00609), which
212 includes also a number of enzymes with decarboxylase or racemase activities. BL23
213 genome encoded 11 hypothetical carboxylases
214 (http://www.ncbi.nlm.nih.gov/genomes/proteins), whether AsdA is a decarboxylase and
215 any of these enzymes would complement its activity, needs to be investigated. A *pepV*
216 mutant strain (BL417) showed a growth pattern similar to the wild-type strain (Fig. 6B),
217 indicating that the hypothetical peptidase encoded by that gene is not essential for the
218 metabolism of 6'FN-Asn. The two genes *asnA2* and *sugK*, present downstream of
219 *pepV*, were however necessary for the utilization of 6'FN-Asn by *L. casei*. An *asnA2*
220 (BL418) mutant strain constructed here and a *sugK* (BL392) mutant previously
221 characterized (41) failed to grow on 6'FN-Asn (Fig. 6C and D). These results indicate
222 that both, the putative glycosylasparaginase AsnA2 and the putative sugar kinase
223 SugK are required for the catabolism of 6'FN-Asn.
224

AsnA2 has glycosylasparaginase activity. The capacity to catabolize 6'FN-Asn by *L. casei* indicated that AsnA2 probably encodes a glycosylasparaginase that would cleave the linkage between GlcNAc and Asn. To confirm this hypothesis, AsnA2 was overexpressed as a His-tagged protein and purified (Fig. S2). The molecular weight of the His-tagged AsnA2 was estimated as 55.6 kDa using size exclusion chromatography, which does not coincide with the theoretical molecular mass (36.071 kDa), suggesting that the enzyme probably forms dimers. Interestingly, when the purified AsnA2 fraction was subjected to SDS-PAGE analysis, three bands were observed, a very faint band at about 38.0 kDa, and two other bands with estimated molecular weights of 18.2 and 17.8 kDa. Mass spectrometry analysis showed that all three protein bands were derived from the glycosylasparaginase AsnA2 (data not shown). The 38 kDa band corresponds to the full-length protein, whereas the 18.2 and 17.8 kDa fragments correspond to the N-terminal and C-terminal domains, respectively. Therefore, AsnA2 is probably a zymogen that is processed during purification. A mechanism of intramolecular autoproteolysis has been previously described for glycosylasparaginases and PNGases (26, 27). The self-processing of the precursor protein occurs at a Thr residue and the two fragments form a non-covalent heterodimeric complex (26). A BLAST search with the amino acid sequence of *L. casei* AsnA2 evidenced a 28% sequence identity to the glycosylasparaginase of *E. meningoseptica* (26). The sequence alignment between both proteins revealed that all residues involved in the autoproteolytic processing, including the catalytic Thr residue (Thr-154 in AsnA2) are conserved. We analyzed the activity of the purified AsnA2 by measuring the release of GlcNAc from GlcNAc-Asn, which confirmed that AsnA2 is a *N*(4)-(β-*N*-acetylglucosaminyl)-L-asparaginase (Fig. S2). This exhibited a specific activity of 20.91 μmol mg protein^{-1} min^{-1} for GlcNAc-Asn. The activity of AsnA2 on the fucosylated glycoamino acid was also tested (Fig. S2). In contrast to the human glycosylasparaginase, which does not act on 6'FN-Asn (48), AsnA2 was able to degrade 6'FN-Asn releasing 6'FN with a specific activity of 0.26 μmol mg protein^{-1} min^{-}

[1]. These results indicated that AsnA2 preferentially acts on GlcNAc-Asn over the fucosylated substrate 6'FN-Asn.

AsdA displays aspartate 4-decarboxylase activity and SugK kinase activity. As described below, the resulting Asp from the activity of AsnA2 on GlcNAc-Asn might be substrate for the AsdA enzyme. To test this hypothesis, AsdA was overexpressed with a His-tag and purified. The recombinant AsdA showed decarboxylation activity on L-Asp with a specific activity of 10.97 ± 2.27 nmol mg protein^{-1} min^{-1}. This weak activity on L-Asp might indicate that this amino acid is not the preferred substrate for AsdA. Regarding SugK, the proposed pathways for 6'FN-Asn and 6'fucosyl-glycans (Fig. 1B) involved the release of the monosaccharides GlcNAc, Glc and Gal, which should be phosphorylated by specific kinases before entering the glycolysis. In order to prove whether SugK showed kinase activity on those sugars, it was overexpressed as a His-tagged protein and purified. SugK displayed kinase activity on GlcNAc (1.44 μmol mg protein^{-1} min^{-1}), but could not phosphorylate Glc and Gal. Activity on *N*-acetylgalactosamine (GalNAc) was also assayed as this *N*-acetylhexosamine is also very abundant on mucosa-associated glycans, and no activity on this sugar was detected.

Proposed pathway for 6'FN-Asn catabolism in *L. casei*. The genetic and biochemical evidence reported here allow proposing a catabolic pathway for 6'FN-Asn in *L. casei* (Fig. 1B). The glycoamino acid is internalized by the permease AlfH, that has a broad specificity over a range of 6´fucosylated substrates, and subsequently defucosylated by the α-L-fucosidase AlfC generating L-fucose and GlcNAc-Asn. The released L-fucose is excreted from the cells by an as yet undetermined mechanism, while GlcNAc-Asn is split by AsnA2 into Asp and 1-amino-GlcNAc, which is unstable and it is non-enzymatically converted to GlcNAc and ammonium (49, 50). The

requirement of AlfC for 6'FN-Asn utilization and the lower affinity of AsnA2 for 6'FN-Asn compared to GlcNAc-Asn supports that the catabolism of 6'FN-Asn occurs through the consecutive action of AlfC and AsnA2. GlcNAc produced by the action of AsnA2 on GlcNAc-Asn would then be the substrate for the sugar kinase SugK (Fig. 1). The other resulting product of AsnA2 activity, Asp, might be the substrate of AsdA, although the weak aspartate 4-decarboxylase activity could indicate that AsdA may play an as yet undetermined role in this pathway. Regarding the function of *pepV*, which encodes a putative peptidase, no signal peptide was evidenced for it, suggesting that it is a cytoplasmic protein. The permease AlfH might also transport more complex substrates, like *N*-glycosylated peptides derived from the proteolysis of host and food-derived proteins. Furthermore, the fact that AlfC is able to release L-fucose from core fucosylation of the Fc fragment from immunoglobulins (51) shows that this enzyme has the capacity to hydrolyze α-1,6 linkages in polypeptidic substrates and could act on core-fucosylated *N*-glycopeptides. In this case, after the release of L-fucose by AlfC, amino acids would be removed by PepV to liberate GlcNAc-Asn (Fig. 1 B).

DISCUSSION

N-glycosylated proteins are present at human mucosal surfaces and breast milk (9, 10, 52), and therefore, they can be accessible to the gut microbiota. Most studies about energy sources for gut beneficial microbes have been focused on carbohydrates present in the diet or added as prebiotics (53) whereas the knowledge about the catabolism of host-derived carbon and nitrogen sources is scarce (16). We have demonstrated that *L. casei* is able to metabolize the glycoamino acid 6'FN-Asn, which is the core structure of the *N*-glycan sites of α1,6-fucosylated glycoproteins. The relevance of the metabolism of this core structure in intestinal microbial ecology has been recently established *in vivo* in humans and in mice models with reduced α1,6 fucosylation of core structures (25). In this work we filled the existing gap relative to the metabolic pathways involved in the utilization of core-fucosylated *N*-glycopeptides by bacteria. The backbone of the *L. casei* 6'FN-Asn pathway consists of the MFS transporter AlfH, the α-L-fucosidase AlfC that removes the α1,6-fucosyl residue, and the glycosylasparaginase AsnA2 that processes the resulting GlcNAc-Asn to 1-amino-GlcNAc and Asp (Fig. 1B). The generated 1-amino-GlcNAc is not metabolizable, but this compound is unstable at acidic pH and it degrades into GlcNAc and ammonium (49). As lactobacilli do not maintain a constant internal pH, but it decreases as the external pH drops (54), intracellular conditions may allow the spontaneous degradation of 1-amino-GlcNAc.The resulting GlcNAc would be then substrate for the sugar kinase SugK, allowing its channeling through glycolysis.

The genetic organization of the *L. casei alf2* gene cluster is well conserved in gene content and gene order across the *L. casei*/*Lactobacillus paracasei*/*Lactobacillus rhamnosus* phylogenetically-related group of lactobacilli, excepting the absence of *asdA* in *L. rhamnosus* (Fig. 7). Homologues of *alfC* are only present in a few *Lactobacillus* species and the closest homologues are harbored by some bifidobacteria isolated from hymenoptera (55-57) (Fig. S3A). Interestingly, many lactobacilli carrying

alfC have also been isolated from insects (58, 59). The phylogenetic analyses of these genes show that they constitute a well-supported cluster together with the *alfC* gene of *Vagococcus humatus*. More distant homologues are mostly present in gut anaerobic bacteria (Fig. S3A). Homologues of *L. casei alfH* are mostly found in the same set of species, although this gene is also present in other bifidobacteria and in *Lactobacillus kisonensis* (Fig. S3B). The genetic association of these genes in these species and their close phylogenetic relationships suggest that they share a common origin and evolutionary history. Homologues of AsnA2 (Fig. S4), AsdA (Fig. S5) and PepV (Fig. S6) are present in numerous lactobacilli. Indeed, *Lactobacillus gasseri* ATCC33323, which carries a gene cluster with *asnA2*, *pepV* and *alfR2* (Fig. 7), has been recently shown to grow with 6´FN and N2F *N*-glycan (25). However, in the same work *L. casei* ATCC334 was reported to use L-fucose, which is contradictory to the fact that no *fuc* genes are present in its genome (60). In addition, *L. casei* ATCC334 was also shown to metabolize 6´FN and N2F *N*-glycan (25), which according to our results in *L. casei* BL23, can only be possible if the repressor *alfR2* is inactivated.

In bifidobacteria, AsnA2 homologs are only present in *Bifidobacterium actinocoloniiforme*, *Bifidobacterium asteroides* and *Bifidobacterium xylocopae* (Fig. S4), and as their AlfC and AlfH counterparts, they are most closely related to *Lactobacillus* sequences. The limited presence in bifidobacteria and the phylogenetic clustering of the three bifidobacterial genes within *Lactobacillus* sequences suggest that they were transferred from *Lactobacillus* to *Bifidobacterium*. Genes encoding PepV homologs are absent in bifidobacteria, whereas *asdA* genes have only been detected in *Bifidobacterium magnum* and *Bifidobacterium gallicum*. The AsdA bifidobacterial sequences constitute a well-supported cluster with sequences from Bacteroidetes and are not closely related to their *Lactobacillus* counterparts (Fig. S5), indicating that they had a different evolutionary origin. Interestingly, closest relatives to *L. casei pepV* are genetically linked to *asnA2* homologs (Fig. 7). This observation suggests a functional link between PepV and AsnA2.

Glycosylasparaginases (E.C. 3.5.1.26) are essential to remove the sugar moiety from the Asn in the GlcNAc-Asn structures derived from *N*-glycoproteins in humans (29, 61). These enzymes cleave the β-aspartylglucosamine linkage and they require both a free α-amino and α-carboxy group on the Asn substrate (29). In lactobacilli, an *asnA2* homolog had been previously identified in *Lactobacillus sakei* as a gene induced during meat (sausage) fermentation, and a knockout mutant resulted in reduced growth on meat, but its activity was not ascertained (64). In contrast to the *Elizabethkingia* glycosylasparaginase, the AsnA2 from *L. casei* characterized here lacks a signal peptide, strongly suggesting that it is an intracellular enzyme. As previously described for glycosylasparaginases, AsnA2 suffers a self-processing proteolytic process to render an active enzyme (Fig. S2). The mature AsnA2 enzyme did not show activity on glycosylated proteins (Fig. S2D), but it showed *in vitro* activity on 6'fucosylated and non-fucosylated GlcNAc-Asn. Curiously, the presence of the linked L-fucose blocks the hydrolysis of 6'FN-Asn by the human glycosylasparaginase (29). However, for the related PNGases it has been demonstrated that the size of the carbohydrate moiety in the substrate has little effect on their activity (62). Therefore AsnA2 would exhibit intermediate characteristics between both types of enzymes: α-1,6-linked L-fucose does not block hydrolysis and the enzyme does not require a glycosylated peptide as substrate.

We had previously characterized the α-L-fucosidase AlfC from *L. casei* (45) and demonstrated that it displays a high regio-specific transglycosylation activity that produces 6'FN disaccharide (47). This enzyme constitutes the only characterized bacterial α-L-fucosidase acting on α-1,6 linkages in core fucosylation structures (core fucosidase) and it has been recently employed as a tool for IgG glycoengineering to obtain defucosylated immunoglobulins with enhanced antibody cell-mediated toxicity (51). Core fucosylation of *N*-glycopeptides and *N*-glycoproteins has also been attained using *L. casei* AlfC mutant enzymes (63). In addition to GlcNAc, we showed here that

AlfC is able to use GlcNAc-Asn, ChbNAc, galactose and glucose as acceptor substrates in transfucosylation reactions. All the synthesized compounds (6'FN-Asn, N2F *N*-glycan, 6'FucGal and 6'FucGlc) have exclusively α-1,6-fucosidic bonds confirming its high linkage specificity. However, the recognition of different acceptors indicates relaxed substrate specificity.

Wild-type *L. casei* did not metabolize the 6'fucosyl-glycans 6'FN, N2F *N*-glycan, 6'FucGal and 6'FucGlc probably due, as shown for 6'FN, to their inability to induce the *alf2* operon. This was confirmed by inactivating *alfR2*, which resulted in constitutive expression of *alf2* genes and subsequent catabolism of those oligosaccharides. Although *alf2* operon induction required the complete glycoamino acid 6'FN-Asn, the coexistence of this and other 6'fucosyl-glycans in environments such as the gastrointestinal tract might allow their simultaneous utilization. Complex networks of cross-feeding between bacteria exist at the gastrointestinal niche and these substrates are probably released in the gut by the concerted action of different microbial enzymes on glycoproteins and other glycocomplexes (21, 23, 24, 64). The results presented here describe the first catabolic route for the utilization of 6'fucosyl-related compounds in bacteria. They support previous works that assign to *N*-glycoproteins a role in nourishing beneficial bacteria in the gut. In addition, they show that commensals and pathogens share related mechanisms to take advantage of host molecules.

MATERIALS AND METHODS

Transfucosylation reactions. AlfC α-L-fucosidase was expressed and purified as previously described (45). Transfucosylation activity of 6x(His)AlfC was also analyzed as previously indicated (47) with some modifications. The reactions mixtures (1 ml) contained 100 mM Tris-HCl buffer, pH 7.0, *p*-nitrophenyl α-L-fucopyranoside (*p*NP-fuc) 50 mM as donor and GlcNAc-Asn (100 mM), *N,N'*-diacetylchitobiose (150 mM), galactose (150 mM) or glucose (150 mM) as acceptors. The mixtures were heated at 98ºC to solubilize the *p*NP-fuc and then were cooled till 42 ºC. Reactions were started by adding 800 U/ml AlfC and after 20 min (reaction with GlcNAc-Asn as acceptor), 15 min (reaction with galactose as acceptor) and 10 min (reactions with *N,N'*-diacetylchitobiose or glucose as acceptors) were heated at 98ºC for 3 min to stop the reaction. The maximum yield obtained for 6'FN-Asn, N2F *N*-glycan, 6'FucGal and 6'FucGlc was 3.6 g/l, 1.8 g/l, 1.3 g/l and 3.3 g/l, respectively. One-dimensional (1D) ^{1}H, 2D ^{1}H, ^{13}C heteronuclear single quantum coherence (HSQC) and 2D heteronuclear multiple-bond correlation (HMBC) NMR analyses demonstrated the exclusive formation of a α1,6-glycosidic linkage between the sugar monomers.

Analytical and semi-preparative HPLC analysis. Transfucosylation reaction products were purified by HPLC using a preparative Rezex RCM-Monosaccharide column (Phenomenex) as previously described (65). Appropriate fractions were pooled, concentrated and analyzed by using an analytical Rezex RSO-oligosaccharide column (Phenomenex) in the case of 6'FN-Asn synthesis and an analytical Rezex RCM-Monosaccharide column (Phenomenex) in the case of N2F *N*-glycan, 6'FucGal and 6'FucGlc synthesis. The synthesized compounds 6'FN-Asn, N2F *N*-glycan, 6'FucGal and 6'FucGlc were subjected to complete hydrolysis with the α-L-fucosidase AlfC and the released L-fucose was measured in order to determine their concentrations.

To determine the glycoamino acids and carbohydrates present in the supernatants from the *Lactobacillus* strain cultures, the bacterial cells were removed by centrifugation, and the cultures were analyzed in a ICS3000 chromatographic system (Dionex) using a CarboPac PA100 column with pulsed amperometric detection. A gradient of 10 mM to 100 mM NaOH was used during 16 min at a flow rate of 1 ml/min.

Nuclear magnetic resonance (NMR) spectroscopy. Samples for NMR were prepared as previously described (66). NMR spectra were also recorded as previously indicated (66) with some modifications. ^{1}H- ^{13}C heteronuclear single quantum coherence (HSQC) experiments were acquired with 360 transients over a spectral width of 10 (for ^{1}H) and 160-220 ppm (for ^{13}C) and 128 points in the indirect dimension. Total correlation spectroscopy (TOCSY) experiments were acquired with 64 transients over a spectral width of 10 ppm in both dimensions and 128 points in the indirect dimension. NMR spectra were processed using the program MesReNoeva 8.1 (Mestrelab Research S.L.).

Bacterial strains and culture conditions. *Lactobacillus* strains (Table 1) were grown at 37ºC under static conditions in MRS medium (Difco). *Escherichia coli* was used as a cloning host and it was routinely grown in Luria-Bertani medium (Oxoid) under shaking at 37 ºC. The corresponding solid media were prepared by adding 1.8 % agar. *L. casei* growth assays with different carbon sources were carried out in MRS basal medium as previously described (41). 6'FN-Asn, 6'FucGal, 6'FucGlc, 6'FN, GlcNAc-Asn, GlcNAc or glucose were added to the MRS basal medium at a concentration of 4 mM, and N2F *N*-glycan was added at 2 mM. Bacterial growth was determined in microtiter plates in a POLARstar Omega plate reader (BMG Labtech). At least three independent biological replicates for each growth curve were obtained and a representative growth curve is shown. For each biological replicate comparing the wild-type and a mutant strain the same batch of MRS basal medium was used. The

concentrations of glycoamino acids and carbohydrates in the culture supernatants at the end of the fermentation were determined by HPLC as described above.

E. coli strains were transformed by electroporation with a Gene Pulser apparatus (Bio-Rad), as recommended by the manufacturer. *E. coli* DH10B transformants were selected with ampicillin (100 μg/ml) and *E. coli* BE50 with ampicillin (100 μg/ml) and kanamycin (50 μg/ml). *L. casei* strains were transformed as described previously (67). *L. casei* transformants were selected with erythromycin (5 μg/ml).

Construction of *L. casei* mutants in *alf2* genes. The *L. casei* BL23 chromosomal DNA was isolated as previously described (67) and used as the template in the PCR reactions that were performed with Expand High Fidelity PCR System (Roche). The *alfR2* gene was amplified by PCR using the primer pair AspDecaFor/XhoPeptVRev2 (Table S3). The resulting 1,289-bp fragment was ligated to pRV300 (68) digested previously with *Eco*RV/*Kpn*I and treated with the Klenow fragment of DNA polymerase I. The obtained plasmid was digested with *Sal*I, ligated and transformed. A clone was selected with a 466-bp deletion in *alfR2* (pRValfR2). DNA fragments containing part of *asdA*, *pepV* and *asnA2* were obtained by PCR using the oligonucleotides pairs: AsdFor/AsdRev, PepVFor/PepVRev and AsnFor/AsnRev, respectively (Table S3) and cloned into pRV300 digested with *Eco*RV. The resulting plasmids pRVasdA, pRVpepV and pRVasnA were cleaved at the unique *Hin*dIII, *Nco*I and *Bcl*I restriction sites present in the *asdA*, *pepV* and *asnA2* coding regions, respectively, to introduce frameshifts in their corresponding coding sequences (Table 1). The three digested plasmids were then treated with Klenow, ligated and transformed into *E. coli* DH10B. The resulting plasmids were transformed in *L. casei* BL23 and the frameshifts introduced into the corresponding genes by a double recombination strategy (41) (Table 1). To construct an *alfC* mutant an internal DNA fragment of *alfC* was obtained by PCR using the oligonucleotides AlfCFor and AlfCRev. The PCR product was cloned into pRV300

digested with *Eco*RV. The resulting plasmid pRValfC was used to transform *L. casei* BL23 and single cross-over integrants were selected by resistance to erythromycin and confirmed by PCR analysis and DNA sequencing. One mutant was selected and named BL415. The same procedure was used to inactivate *alfC* in the mutant strain BL405 (*alfR2*) obtaining the double mutant *alfR2 alfC* (strain BL406). To contruct the double mutants *alfR2 alfH* (strain BL407), the plasmid pRValfH was generated (Table 1). A DNA fragment containing part of *alfH* was obtained with the oligonucleotide pair FucPerFor/FucPerRev and cloned into pRV300 digested with *Eco*RV. The resulting plasmid pRValfH was cleaved at the unique *Bcl*I restriction site present in the *alfH* coding region, treated with Klenow, ligated and transformed. A construct was selected in which a frameshift was introduced at the *Bcl*I site in *alfH* (pRValfH). pRValfH was transformed in the mutant strain BL405 (*alfR2*). A clone having a second recombination event was selected to obtain the double mutant *alfR2 alfH* (strain BL407).

Sequence analysis. DNA sequencing was carried out by the Central Service of Research Support of the University of Valencia (Spain). M13 universal and reverse primers or custom primers hybridizing within the appropriate DNA fragments were used for sequencing. Sequence analyses were carried out with DNAMAN 4.03 for Windows (Lynnon BioSoft) and sequence similarities were analyzed with the BLAST program (69). Genomic context analysis was performed at the *Microbial Genome Database for Comparative Analysis (*MBGD) (http://mbgd.genome.ad.jp/) (70).

Reverse transcription-quantitative PCR analysis (RT-qPCR). Total RNA was isolated from *L. casei* strains BL23 (WT) and BL405 (*alfR2*) grown in MRS basal medium supplemented with 4 mM of different glycans (6'FN-Asn, 6'FN, GlcNAc or Glucose) as previously described (41) . The isolated RNA was digested with DNaseI and retro-transcribed using the Maxima First strand cDNA Synthesis Kit (Fermentas) (41). RT-qPCR was performed for each cDNA sample in triplicate using the Lightcycler

480 system (Roche), LC Fast Start DNA Master SYBR green I (Roche) and the primers pairs: q29280for/q29280rev (*sugK*), q29290for/q29290rev (*asnA2*), q29300for/q29300rev (*pepV*) and q29310for/q29310rev (*alfR2*), q29320for/q29320rev (*asdA*), q29330for/q29330rev (*alfH*) and q29340for/q29340rev (*alfC*) (Table S3). The reaction mixtures and cycling conditions were performed as previously described (41). The *pyrG*, *lepA* and *IleS* genes were chosen as reference genes (71). Relative expression values were calculated using the software tool REST (relative expression software tool) (72). Linearity and amplification efficiency were determined for each primer pair.

Expression and purification of AsnA2, AsdA and SugK. The coding regions of *asnA2, asdA* and *SugK* were amplified by PCR using the pair primers AsnHindIIFor/AsnBamHIRev, AsdAHCt-F/AsdAHCt-R and SugKBamH1For/SugKRev, respectively (Table S3). AsnA2 was cloned into *Hind*III - *Bam*HI sites and SugK was cloned in the *Bam*HI - *Sma*I sites of the pQE80 vector and transformed into *E. coli* BE50 co-expressing chaperones *GroES* and *GroEL*. pETasdA was constructed using the Gibson assembly kit (NEB) with the *asdA* PCR fragment and pET28a(+) digested with *Nco*I and *Xho*I. pETasdA was transformed into *E. coli* BL21(DE3)pLys. For purification, cells were grown to OD_{600} of 0.8, 1 mM isopropyl-β-d-thiogalactopyranoside was added, and incubation was continued at 25°C for 10 h. Bacterial cells extracts were loaded onto a HisTrap column (GE Healthcare), and His-tagged protein was purified according to the supplier's recommendations. The native molecular weight of the AsnA2 protein was estimated by size exclusion chromatography (HiPrep 16/60 Sephacryl S-300 HR column).

Mass Spectrometry analysis. Protein bands from AsnA2 purification were excised from the gel, trypsinized, and analyzed in a 5800 MALDI TOF/TOF system (AB Sciex)

532 at the proteomics service of the University of Valencia. MS and MS/MS data were
533 analyzed with the Mascot server.
534
535 **AsnA2 enzyme activity**. The activity of the purified AsnA2 enzyme was assayed at
536 37ºC with GlcNAc-Asn and 6'FN-Asn as substrates. The released GlcNAc and 6'FN,
537 respectively, were quantified by analyzing the reaction mixtures by ionic
538 chromatography (Dionex) as described above. Reaction mixtures (20 μl) containing 5
539 mM substrate in 100 mM Tris-HCl buffer, pH 7.0, were initiated by adding 0.2 μg of
540 enzyme. Protein deglycosylation assays were performed with reaction mixtures (15 μl)
541 containing 3.75 μg of ovalbumin or lactoferrin in 100 mM Tris-HCl buffer, pH 7.0. The
542 reactions were initiated with 0.2 μg of enzyme and incubated at 37ºC overnight.
543
544 **AsdA enzyme activity.** AsdA decarboxylase activity on L-Asp was measured as
545 previously described with some modifications (73). The resulting L-Ala was determined
546 by using a coupled enzyme assay. Reaction mixtures (100 µl) containing 100 mM K-
547 acetate buffer (pH 5.5), 0.2 mM pyridoxal 5-phosphate, 1 mM α-ketoglutarate, 0.4 mM
548 NAD^+, 0.32 U of L-alanine dehydrogenase (Sigma) and 10 µg of AsdA, were initiated
549 by addition of 40 mM of L-Asp. Reactions were incubated for 60 min at 37°C and the
550 production of NADH was monitored at 340 nm.
551
552 **SugK enzyme activity**. SugK phosphorylation activity on different sugars was
553 determined by using a coupled enzyme assay as previously described (74). Reaction
554 mixtures (100 µl) containing 100 mM Tris-HCl (pH 7.5), 10 mM $MgCl_2$, 5 mM ATP, 1
555 mM phosphoenolpyruvate, 0.2 mM NADH, 10 U of pyruvate kinase, 7 U of lactate
556 dehydrogenase and various substrates (GlcNAc, Glc, Gal or GalNAc) at a final
557 concentration of 1 mM, were initiated by addition of 0.75 µg of SugK. Reactions were
558 incubated for 15 min at 37°C and NADH formation was monitored at 340 nm.

559

560 **Phylogenetic analysis.** Sequences of *alfC*, *alfH*, *asnA2*, *asdA* and *pepV*
561 homologues were retrieved from the microbial genome repository at the NCBI by
562 BLAST (75) using as query sequences their corresponding *L. casei* BL23 protein
563 sequences. For *asnA2*, only sequences from *Lactobacillaceae* and *Bifidobacteriaceae*
564 were included. Domain analysis was performed using the tools implemented at the
565 NCBI Blast site (https://blast.ncbi.nlm.nih.gov/Blast.cgi). The resulting datasets were
566 aligned with M-Coffee (76) at the T-Coffee server (http://tcoffee.crg.cat) with default
567 settings. Positions of uncertain homology and gaps were removed using GBLOCKS
568 (77) at the Gblocks server (http://molevol.cmima.csic.es/castresana/
569 Gblocks_server.html) allowing smaller final blocks and less strict flanking positions.
570 Redundant sequences were removed by using the EMBOSS suite Skipredundant tool
571 (78) with a percentage sequence identity redundancy threshold of 98%. The best-fit
572 models of amino acid substitution and maximum likelihood trees were obtained using
573 PhyML ver. 3.0 (79) at the PhyML server (http://www.atgc-montpellier.fr/phyml).
574 Bootstrap support values were obtained from 1000 pseudorandom replicates.
575

576 **Statistical analysis**. Student's *t*-test was performed using Statgraphics Plus,
577 version 2.1 (Statistical Graphics Corp., USA) and it was used to detect statistically
578 significant differences between final O.D. values reached by *L. casei* BL405 (*alfR2*)
579 cultures versus each mutant BL406 (*alfR2 alfC*) and BL407 (*alfR2 alfH*) strains.
580 Statistical significance was accepted at $P < 0.05$.
581

582 **ACKNOWLEDGEMENTS**

583 This work was financed by funds of the Spanish Ministry for Economy and
584 Competitiveness (MINECO)/FEDER through the Project AGL2014-52996-C2 (1-R and
585 2-R) and AGL2017-84165-C2 (1-R and 2-R). J.E.B. was supported by a Santiago
586 Grisolía predoctoral fellowship from the Valencian Government. J.R-D. was supported
587 by a Ramon y Cajal Contract by the Spanish Ministry for Economy and
588 Competitiveness. R.G-R was recipient of a postdoctoral fellowship from the Generalitat
589 Valenciana that was cofounded by the European Social Fund. Part of the equipment
590 employed in this work has been funded by Generalitat Valenciana and co-financed with
591 ERDF funds (OP ERDF of Comunitat Valenciana 2014-2020).

REFERENCES

1. Chen W, Liu F, Ling Z, Tong X, Xiang C. 2012. Human intestinal lumen and mucosa-associated microbiota in patients with colorectal cancer. PLoS One 7:e39743.
2. Chen SJ, Liu XW, Liu JP, Yang XY, Lu FG. 2014. Ulcerative colitis as a polymicrobial infection characterized by sustained broken mucus barrier. World J Gastroenterol 20:9468-9475.
3. Blander JM, Longman RS, Iliev ID, Sonnenberg GF, Artis D. 2017. Regulation of inflammation by microbiota interactions with the host. Nat Immunol 18:851-860.
4. Leyer GJ, Li S, Mubasher ME, Reifer C, Ouwehand AC. 2009. Probiotic effects on cold and influenza-like symptom incidence and duration in children. Pediatrics 124:e172-9.
5. Tokuhara D, Kurashima Y, Kamioka M, Nakayama T, Ernst P, Kiyono H. 2019. A comprehensive understanding of the gut mucosal immune system in allergic inflammation. Allergol Int 68:17-25.
6. Thursby E, Juge N. 2017. Introduction to the human gut microbiota. Biochem J 474:1823-1836.
7. Apweiler R, Hermjakob H, Sharon N. 1999. On the frequency of protein glycosylation, as deduced from analysis of the SWISS-PROT database. Biochim Biophys Acta 1473:4-8.
8. Krasnova L, Wong CH. 2016. Exploring human glycosylation for better therapies. Mol Aspects Med 51:125-143.
9. Park D, Xu G, Barboza M, Shah IM, Wong M, Raybould H, Mills DA, Lebrilla CB. 2017. Enterocyte glycosylation is responsive to changes in extracellular conditions: implications for membrane functions. Glycobiology 27:847-860.

10. Picariello G, Ferranti P, Mamone G, Roepstorff P, Addeo F. 2008. Identification of N-linked glycoproteins in human milk by hydrophilic interaction liquid chromatography and mass spectrometry. Proteomics 8:3833-3847.
11. Yang Y, Zheng N, Zhao X, Zhang Y, Han R, Zhao S, Yang J, Li S, Guo T, Zang C, Wang J. 2017. N-glycosylation proteomic characterization and cross-species comparison of milk whey proteins from dairy animals. Proteomics 17.
12. Imperiali B, Hendrickson TL. 1995. Asparagine-linked glycosylation: specificity and function of oligosaccharyl transferase. Bioorg Med Chem 3:1565-1578.
13. Ohtsubo K, Marth JD. 2006. Glycosylation in cellular mechanisms of health and disease. Cell 126:855-867.
14. Lyons JJ, Milner JD, Rosenzweig SD. 2015. Glycans Instructing Immunity: The emerging role of altered glycosylation in clinical immunology. Front Pediatr 3:54.
15. Mathias A, Corthesy B. 2011. Recognition of gram-positive intestinal bacteria by hybridoma- and colostrum-derived secretory immunoglobulin A is mediated by carbohydrates. J Biol Chem 286:17239-41727.
16. Zuniga M, Monedero V, Yebra MJ. 2018. Utilization of host-derived glycans by intestinal *Lactobacillus* and *Bifidobacterium* Species. Front Microbiol 9:1917.
17. Koropatkin NM, Cameron EA, Martens EC. 2012. How glycan metabolism shapes the human gut microbiota. Nat Rev Microbiol 10:323-335.
18. Fairbanks AJ. 2017. The ENGases: versatile biocatalysts for the production of homogeneous N-linked glycopeptides and glycoproteins. Chem Soc Rev 46:5128-5146.
19. Collin M, Shannon O, Bjorck L. 2008. IgG glycan hydrolysis by a bacterial enzyme as a therapy against autoimmune conditions. Proc Natl Acad Sci U S A 105:4265-4270.

20. Renzi F, Manfredi P, Mally M, Moes S, Jeno P, Cornelis GR. 2011. The N-glycan glycoprotein deglycosylation complex (Gpd) from *Capnocytophaga canimorsus* deglycosylates human IgG. PLoS Pathog 7:e1002118.
21. Garbe J, Sjogren J, Cosgrave EF, Struwe WB, Bober M, Olin AI, Rudd PM, Collin M. 2014. EndoE from *Enterococcus faecalis* hydrolyzes the glycans of the biofilm inhibiting protein lactoferrin and mediates growth. PLoS One 9:e91035.
22. Robb M, Hobbs JK, Woodiga SA, Shapiro-Ward S, Suits MD, McGregor N, Brumer H, Yesilkaya H, King SJ, Boraston AB. 2017. Molecular Characterization of N-glycan Degradation and Transport in *Streptococcus pneumoniae* and its contribution to virulence. PLoS Pathog 13:e1006090.
23. Garrido D, Nwosu C, Ruiz-Moyano S, Aldredge D, German JB, Lebrilla CB, Mills DA. 2012. Endo-beta-N-acetylglucosaminidases from infant gut-associated bifidobacteria release complex N-glycans from human milk glycoproteins. Mol Cell Proteomics 11:775-785.
24. Parc AL, Karav S, De Moura Bell J, Frese SA, Liu Y, Mills DA, Block DE, Barile D. 2015. A novel endo-beta-N-acetylglucosaminidase releases specific N-glycans depending on different reaction conditions. Biotechnol Prog 31:1323-1330.
25. Li M, Bai Y, Zhou J, Huang W, Yan J, Tao J, Fan Q, Liu Y, Mei D, Yan Q, Yuan J, Malard P, Wang Z, Gu J, Tanigchi N, Li W. 2019. Core fucosylation of maternal milk N-glycan evokes B cell activation by selectively promoting the L-fucose metabolism of gut *Bifidobacterium* spp. and *Lactobacillus* spp. mBio 10.
26. Wang Y, Guo HC. 2010. Crystallographic snapshot of glycosylasparaginase precursor poised for autoprocessing. J Mol Biol 403:120-130.
27. Witte MD, van der Marel GA, Aerts JM, Overkleeft HS. 2011. Irreversible inhibitors and activity-based probes as research tools in chemical glycobiology. Org Biomol Chem 9:5908-5926.

672 28. Fan JQ, Lee YC. 1997. Detailed studies on substrate structure requirements of
673 glycoamidases A and F. J Biol Chem 272:27058-27064.
674 29. Risley JM, Huang DH, Kaylor JJ, Malik JJ, Xia YQ, York WM. 2001.
675 Glycosylasparaginase activity requires the alpha-carboxyl group, but not the
676 alpha-amino group, on N(4)-(2-Acetamido-2-deoxy-beta-D-glucopyranosyl)-L-
677 asparagine. Arch Biochem Biophys 391:165-170.
678 30. Tarentino AL, Plummer TH, Jr. 1993. The first demonstration of a procaryotic
679 glycosylasparaginase. Biochem Biophys Res Commun 197:179-186.
680 31. Sun G, Yu X, Bao C, Wang L, Li M, Gan J, Qu D, Ma J, Chen L. 2015.
681 Identification and characterization of a novel prokaryotic peptide: N-glycosidase
682 from *Elizabethkingia meningoseptica*. J Biol Chem 290:7452-7462.
683 32. Wang T, Cai ZP, Gu XQ, Ma HY, Du YM, Huang K, Voglmeir J, Liu L. 2014.
684 Discovery and characterization of a novel extremely acidic bacterial N-
685 glycanase with combined advantages of PNGase F and A. Biosci Rep
686 34:e00149.
687 33. Guo HC, Xu Q, Buckley D, Guan C. 1998. Crystal structures of Flavobacterium
688 glycosylasparaginase. An N-terminal nucleophile hydrolase activated by
689 intramolecular proteolysis. J Biol Chem 273:20205-20212.
690 34. Tarentino AL, Quinones G, Hauer CR, Changchien LM, Plummer TH, Jr. 1995.
691 Molecular cloning and sequence analysis of *Flavobacterium meningosepticum*
692 glycosylasparaginase: a single gene encodes the alpha and beta subunits. Arch
693 Biochem Biophys 316:399-406.
694 35. Tuohy KM, Pinart-Gilberga M, Jones M, Hoyles L, McCartney AL, Gibson GR.
695 2007. Survivability of a probiotic *Lactobacillus casei* in the gastrointestinal tract
696 of healthy human volunteers and its impact on the faecal microflora. J Appl
697 Microbiol 102:1026-1032.
698 36. Radicioni M, Koirala R, Fiore W, Leuratti C, Guglielmetti S, Arioli S. 2018.
699 Survival of *L. casei* DG((R)) (*Lactobacillus paracasei* CNCMI1572) in the

gastrointestinal tract of a healthy paediatric population. Eur J Nutr doi:10.1007/s00394-018-1860-1865.

37. Rubio R, Jofre A, Martin B, Aymerich T, Garriga M. 2014. Characterization of lactic acid bacteria isolated from infant faeces as potential probiotic starter cultures for fermented sausages. Food Microbiol 38:303-311.

38. Mansour NM, Heine H, Abdou SM, Shenana ME, Zakaria MK, El-Diwany A. 2014. Isolation of *Enterococcus faecium* NM113, *Enterococcus faecium* NM213 and *Lactobacillus casei* NM512 as novel probiotics with immunomodulatory properties. Microbiol Immunol 58:559-569.

39. Hill D, Sugrue I, Tobin C, Hill C, Stanton C, Ross RP. 2018. The *Lactobacillus casei* group: history and health related applications. Front Microbiol 9:2107.

40. McFarland LV, Evans CT, Goldstein EJC. 2018. Strain-specificity and disease-specificity of srobiotic efficacy: a systematic review and meta-analysis. Front Med (Lausanne) 5:124.

41. Bidart GN, Rodriguez-Diaz J, Monedero V, Yebra MJ. 2014. A unique gene cluster for the utilization of the mucosal and human milk-associated glycans galacto-N-biose and lacto-N-biose in *Lactobacillus casei*. Mol Microbiol 93:521-538.

42. Bidart GN, Rodriguez-Diaz J, Perez-Martinez G, Yebra MJ. 2018. The lactose operon from *Lactobacillus casei* is involved in the transport and metabolism of the human milk oligosaccharide core-2 N-acetyllactosamine. Sci Rep 8:7152.

43. Bidart GN, Rodriguez-Diaz J, Yebra MJ. 2016. The Extracellular wall-bound beta-N-acetylglucosaminidase from *Lactobacillus casei* Is Involved in the metabolism of the human milk oligosaccharide Lacto-N-Triose. Appl Environ Microbiol 82:570-577.

44. Rodriguez-Diaz J, Rubio-del-Campo A, Yebra MJ. 2012. *Lactobacillus casei* ferments the N-Acetylglucosamine moiety of fucosyl-alpha-1,3-N-

727 acetylglucosamine and excretes L-fucose. Appl Environ Microbiol 78:4613-
728 4619.
729 45. Rodriguez-Diaz J, Monedero V, Yebra MJ. 2011. Utilization of natural
730 fucosylated oligosaccharides by three novel alpha-L-fucosidases from a
731 probiotic *Lactobacillus casei* strain. Appl Environ Microbiol 77:703-705.
732 46. Maze A, Boel G, Zuniga M, Bourand A, Loux V, Yebra MJ, Monedero V, Correia
733 K, Jacques N, Beaufils S, Poncet S, Joyet P, Milohanic E, Casaregola S,
734 Auffray Y, Perez-Martinez G, Gibrat JF, Zagorec M, Francke C, Hartke A,
735 Deutscher J. 2010. Complete genome sequence of the probiotic *Lactobacillus*
736 *casei* strain BL23. J Bacteriol 192:2647-2648.
737 47. Rodriguez-Diaz J, Carbajo RJ, Pineda-Lucena A, Monedero V, Yebra MJ. 2013.
738 Synthesis of fucosyl-N-acetylglucosamine disaccharides by transfucosylation
739 using alpha-L-fucosidases from *Lactobacillus casei*. Appl Environ Microbiol
740 79:3847-3850.
741 48. Noronkoski T, Mononen I. 1997. Influence of L-fucose attached alpha 1-->6 to
742 the asparagine-linked N-acetylglucosamine on the hydrolysis of the N-glycosidic
743 linkage by human glycosylasparaginase. Glycobiology 7:217-220.
744 49. Makino M, Kojima T, Ohgushi T, Yamashina I. 1968. Studies on enzymes
745 acting on glycopeptides. J Biochem 63:186-192.
746 50. Aronson NN, Jr. 1999. Aspartylglycosaminuria: biochemistry and molecular
747 biology. Biochim Biophys Acta 1455:139-154.
748 51. Giddens JP, Lomino JV, DiLillo DJ, Ravetch JV, Wang LX. 2018. Site-selective
749 chemoenzymatic glycoengineering of Fab and Fc glycans of a therapeutic
750 antibody. Proc Natl Acad Sci U S A 115:12023-12027.
751 52. Froehlich JW, Dodds ED, Barboza M, McJimpsey EL, Seipert RR, Francis J, An
752 HJ, Freeman S, German JB, Lebrilla CB. 2010. Glycoprotein expression in
753 human milk during lactation. J Agric Food Chem 58:6440-6448.

754 53. Holscher HD. 2017. Dietary fiber and prebiotics and the gastrointestinal
755 microbiota. Gut Microbes 8:172-184.
756 54. Kashket ER. 1987. Bioenergetics of lactic acid bacteria: cytoplasmic pH and
757 osmotolerance. FEMS Microbiol Rev 46:233-244.
758 55. Killer J, Kopecny J, Mrazek J, Koppova I, Havlik J, Benada O, Kott T. 2011.
759 *Bifidobacterium actinocoloniiforme* sp. nov. and *Bifidobacterium bohemicum* sp.
760 nov., from the bumblebee digestive tract. Int J Syst Evol Microbiol 61:1315-
761 1321.
762 56. Scardovi V, Trovatelli LD. 1969. New species of bifid bacteria from *Apis*
763 *mellifica* L. and *Apis indica* F. A contribution to the taxonomy and biochemistry
764 of the genus *Bifidobacterium*. Zentralbl Bakteriol Parasitenkd Infektionskr Hyg
765 123:64-88.
766 57. Alberoni D, Gaggia F, Baffoni L, Modesto MM, Biavati B, Di Gioia D. 2019.
767 *Bifidobacterium xylocopae* sp. nov. and *Bifidobacterium aemilianum* sp. nov.,
768 from the carpenter bee (*Xylocopa violacea*) digestive tract. Syst Appl Microbiol
769 42:205-216.
770 58. Olofsson TC, Alsterfjord M, Nilson B, Butler E, Vasquez A. 2014. *Lactobacillus*
771 *apinorum* sp. nov., *Lactobacillus mellifer* sp. nov., *Lactobacillus mellis* sp. nov.,
772 *Lactobacillus melliventris* sp. nov., *Lactobacillus kimbladii* sp. nov.,
773 *Lactobacillus helsingborgensis* sp. nov. and *Lactobacillus kullabergensis* sp.
774 nov., isolated from the honey stomach of the honeybee *Apis mellifera*. Int J Syst
775 Evol Microbiol 64:3109-3119.
776 59. Killer J, Votavova A, Valterova I, Vlkova E, Rada V, Hroncova Z. 2014.
777 *Lactobacillus bombi* sp. nov., from the digestive tract of laboratory-reared
778 bumblebee queens (*Bombus terrestris*). Int J Syst Evol Microbiol 64:2611-2617.
779 60. Vinay-Lara E, Hamilton JJ, Stahl B, Broadbent JR, Reed JL, Steele JL. 2014.
780 Genome-scale reconstruction of metabolic networks of *Lactobacillus casei*
781 ATCC 334 and 12A. PLoS One 9:e110785.

782 61. Arvio M, Mononen I. 2016. Aspartylglycosaminuria: a review. Orphanet J Rare
783 Dis 11:162.
784 62. Altmann F, Schweiszer S, Weber C. 1995. Kinetic comparison of peptide: N-
785 glycosidases F and A reveals several differences in substrate specificity.
786 Glycoconj J 12:84-93.
787 63. Li C, Zhu S, Ma C, Wang LX. 2017. Designer alpha1,6-Fucosidase Mutants
788 Enable Direct Core Fucosylation of Intact N-Glycopeptides and N-
789 Glycoproteins. J Am Chem Soc 139:15074-15087.
790 64. Carroll IM, Maharshak N. 2013. Enteric bacterial proteases in inflammatory
791 bowel disease- pathophysiology and clinical implications. World J Gastroenterol
792 19:7531-43.
793 65. Becerra JE, Coll-Marques JM, Rodriguez-Diaz J, Monedero V, Yebra MJ. 2015.
794 Preparative scale purification of fucosyl-N-acetylglucosamine disaccharides and
795 their evaluation as potential prebiotics and antiadhesins. Appl Microbiol
796 Biotechnol 99:7165-7176.
797 66. Bidart GN, Rodriguez-Diaz J, Palomino-Schatzlein M, Monedero V, Yebra MJ.
798 2017. Human milk and mucosal lacto- and galacto-N-biose synthesis by
799 transgalactosylation and their prebiotic potential in *Lactobacillus* species. Appl
800 Microbiol Biotechnol 101:205-215.
801 67. Posno M, Leer RJ, van Luijk N, van Giezen MJ, Heuvelmans PT, Lokman BC,
802 Pouwels PH. 1991. Incompatibility of *Lactobacillus* vectors with replicons
803 derived from small cryptic *Lactobacillus* plasmids and segregational instability of
804 the introduced vectors. Appl Environ Microbiol 57:1822-1828.
805 68. Leloup L, Ehrlich SD, Zagorec M, Morel-Deville F. 1997. Single-crossover
806 integration in the *Lactobacillus sake* chromosome and insertional inactivation of
807 the ptsI and lacL genes. Appl Environ Microbiol 63:2117-2123.
808 69. Altschul SF, Gish W, Miller W, Myers EW, Lipman DJ. 1990. Basic local
809 alignment search tool. J Mol Biol 215:403-410.

70. Uchiyama I, Higuchi T, Kawai M. 2010. MBGD update 2010: toward a comprehensive resource for exploring microbial genome diversity. Nucleic Acids Res 38:D361-365.

71. Landete JM, Garcia-Haro L, Blasco A, Manzanares P, Berbegal C, Monedero V, Zuniga M. 2010. Requirement of the *Lactobacillus casei* MaeKR two-component system for L-malic acid utilization via a malic enzyme pathway. Appl Environ Microbiol 76:84-95.

72. Pfaffl MW, Horgan GW, Dempfle L. 2002. Relative expression software tool (REST) for group-wise comparison and statistical analysis of relative expression results in real-time PCR. Nucleic Acids Res 30:e36.

73. Wang NC, Lee CY. 2006. Molecular cloning of the aspartate 4-decarboxylase gene from *Pseudomonas* sp. ATCC 19121 and characterization of the bifunctional recombinant enzyme. Appl Microbiol Biotechnol 73:339-348.

74. Reith J, Berking A, Mayer C. 2011. Characterization of an N-acetylmuramic acid/N-acetylglucosamine kinase of *Clostridium acetobutylicum*. J Bacteriol 193:5386-5392.

75. Altschul SF, Madden TL, Schäffer AA, Zhang J, Zhang Z, Miller W, Lipman DJ. 1997. Gapped BLAST and PSI-BLAST: a new generation of protein database search programs. Nucleic Acids Research 25:3389-3402.

76. Notredame C, Higgins DG, Heringa J. 2000. T-coffee: a novel method for fast and accurate multiple sequence alignment11Edited by J. Thornton. Journal of Molecular Biology 302:205-217.

77. Castresana J. 2000. Selection of conserved blocks from multiple alignments for their use in phylogenetic analysis. Molecular Biology and Evolution 17:540-552.

78. Rice P, Longden I, Bleasby A. 2000. EMBOSS: The European Molecular Biology Open Software Suite. Trends in Genetics 16:276-277.

79. Guindon S, Gascuel O. 2003. A simple, fast, and accurate algorithm to estimate large phylogenies by maximum likelihood. Systematic Biology 52:696-704.

80. Dale GE, Schonfeld HJ, Langen H, Stieger M. 1994. Increased solubility of trimethoprim-resistant type S1 DHFR from *Staphylococcus aureus* in *Escherichia coli* cells overproducing the chaperonins GroEL and GroES. Protein Eng 7:925-931.

844 **Table 1**. Strains and plasmids used in this study

Strain or plasmid	Relevant genotype or properties	Source or
Strains		
Lactobacillus casei		
BL23	Wild type	CECT 5275
BL372	BL23 *alfH::*pRV300 Erm^R	(44)
BL392	BL23 *sugK::*pRV300 Erm^R	(41)
BL405	BL23 *alfR2* (466-bp internal deletion at *alfR2*)	This work
BL406	BL23 *alfR2alfC* (466-bp internal deletion at *alfR2* and *alfC::* pRV300 Erm^R)	This work
BL407	BL23 *alfR2alfH* (466-bp internal deletion at *alfR2* and frameshift in *alfH* at *BclI* site)	This work
BL415	BL23 *alfC::*pRV300 Erm^R	This work
BL416	BL23 *asdA* (frameshift at *Hind*III site)	This work
BL417	BL23 *pepV* (frameshift at *Nco*I site)	This work
BL418	BL23 *asnA2* (frameshift at *Bcl*I site)	This work
Escherichia coli		
DH10B	F^- *endA1 recA1 galE15 galK16 nupG rpsL* Δlac*X74* Φ80l*acZ*ΔM15 *araD139* Δ(*ara,leu*)7697 *mcrA* Δ(*mrr-*h*sdRMS-mcrBC*) λ^-	Invitrogen
GM119	F^-*supE44*, *lacY1*, *galK2*, *galT22*, *metB1*, *dcm-6*, *dam-3*, *tsx-78* λ^-	ATCC53339
BE50	BL21(DE3) containing pREPGroES/GroEL	(80)
PE149	DH10B containing pQEalfC	(45)
PE173	BE50 containing pQEasnA2	This work
PE174	BL21(DE3)pLys containing pETasdA	This work
PE176	BE50 containing pQEsugK	This work
Plasmids		
pRV300	Suicide vector carrying Erm^R from pAMβ1	(68)
pRValfR2	pRV300 with a fragment carrying a 466-bp deletion at the *alfR2*-coding region	This work
pRVasdA	pRV300 with a frameshift at *Hind*III site in *asdA* fragment	This work
pRVpepV	pRV300 with a frameshift at *Nco*I site in *pepV* fragment	This work
pRVasnA	pRV300 with a frameshift at *Bcl*I site in *ansA* fragment	This work
pRValfC	pRV300 with a 669–bp *alfC* fragment	This work
pRValfH	pRV300 with a frameshift at *Bcl*I site in *alfH* fragment	This work
pQE80	*E. coli* expression vector; Amp^R	Qiagen
pET-28a(+)	*E. coli* expression vector, Kan^R	Novogen
pQEasnA2	pQE80 containing *asnA2*-coding region	This work
pETasdA	pET-28a(+) containing *asdA*-coding region	This work
pQEsugK	pQE80 containing *sugK*-coding region	This work

845 CECT, Colección Española de Cultivos Tipo; Erm^R, erythromycin resistant; Amp^R, ampicillin resistant ;
846 Kan^R, kanamycin resistant

847 **FIGURE LEGENDS**

848

849 **Figure 1**. (A) Structural organization of the *Lactobacillus casei* BL23 *alf2* operon. (B)
850 Schematic presentation of the transport and catabolic pathways for fucosyl-α-1,6-*N*-
851 acetylglucosamine-asparagine, fucosylated glycans (fucosyl-α-1,6-*N*-
852 acetylglucosamine, fucosyl-α-1,6-glucose, fucosyl-α-1,6-galactose and fucosyl-α-1,6-
853 *N*,*N*'-diacetylchitobiose) and fucosylated *N*-glycopeptides in *Lactobacillus casei*. AlfC,
854 α-L-fucosidase AlfC; AsnA2, *N*(4)-(β-*N*-acetylglucosaminyl)-L-asparaginase; AsdA,
855 aspartate 4-decarboxylase; PepV, peptidase V; SugK, sugar kinase.

856

857 **Figure 2**. ^{1}H NMR spectra of compounds in D_2O acquired at 27 ºC and 600 MHz with
858 an inverse cryoprobe. A) fucosyl-α-1,6-*N*-acetylglucosamine-asparagine (6'FN-Asn); B)
859 fucosyl-α-1,6-*N*,*N*'-diacetylchitobiose (N2F *N*-glycan); C) fucosyl-α-1,6-galactose
860 (6'FucGal); D) fucosyl-α-1,6-glucose (6'FucGlc). Signals labelled with Fu correspond to
861 copurified L-fucose.

862

863 **Figure 3**. Growth profiles of *Lactobacillus casei* on *N*-glycan derivatives. *L. casei* wild-
864 type strain BL23 (A) and strain BL405, an *alfR2* deletion mutant (B) grown on MRS
865 basal medium without carbon source (black squares), with fucosyl-α-1,6-*N*-
866 acetylglucosamine-asparagine (6'FN-Asn) (green circles), fucosyl-α-1,6-*N*-
867 acetylglucosamine (6'FN) (red diamonds), *N*-acetylglucosamine-asparagine (GlcNAc-
868 Asn) (blue hexagons), fucosyl-α-1,6-glucose (6'FucGlc) (pink triangles), fucosyl-α-1,6-
869 galactose (6'FucGal) (cyan crosses) or fucosyl-α-1,6-*N*,*N*'-diacetylchitobiose (N2F *N*-
870 glycan) (grey x). (C) HPLC chromatograms (Dionex system) of the standard
871 compounds L-fucose 0.25 mM (1), fucosyl-α-1,6-*N*-acetylglucosamine (6'FN) 0.2 mM
872 (2), fucosyl-α-1,6-*N*,*N*'-diacetylchitobiose (N2F *N*-glycan) 0.2 mM (3), fucosyl-α-1,6-
873 glucose (6'FucGlc) 0.2 mM (4) and fucosyl-α-1,6-galactose (6'FucGal) 0.2 mM (5) and

culture supernatants (20 times diluted) from *L. casei* BL23 (WT) (6, 8,10,12, 14) and BL405 (*alfR2*) (7,9,11, 13, 15) grown in 6'FN (6,7), 6'FucGlc (8,9), 6'FucGal (10,11), N2F *N*-glycan (12,13) and without sugar (14,15). The numbers by the L-fucose peaks indicated the concentration in mM.

Figure 4. Expression of *alf2* genes in *Lactobacillus casei*. *L. casei* BL23 (WT) and *L. casei* BL405 (*alfR2* deletion mutant) were grown in MRS basal medium containing fucosyl-α-1,6-*N*-acetylglucosamine-asparagine (6'FN-Asn), fucosyl-α-1,6-*N*-acetylglucosamine (6'FN) or *N*-aceylglucosamine (GlcNAc). Gene expression in *L. casei* BL405 in the presence of glucose is also shown. The expression was monitored by RT-qPCR and *L. casei* BL23 (WT) cells grown in MRS basal medium with glucose were used as reference condition. Data presented are mean values based on at least three replicates. Bars indicate standard errors.

Figure 5. Growth curves of *Lactobacillus casei* mutant strains. BL415 (*alfC*) (A) and BL372 (*alfH*) (B) on MRS basal medium without carbon source (black squares), with fucosyl-α-1,6-*N*-acetylglucosamine-asparagine (6'FN-Asn) (green circles) or *N*-acetylglucosamine (GlcNAc) (blue triangles down). BL406 (*alfR2alfC*) (C) and BL407 (*alfR2alfH*) (D) on MRS basal medium without carbon source (black squares), with fucosyl-α-1,6-*N*-acetylglucosamine-asparagine (6'FN-Asn) (green circles), fucosyl-α-1,6-*N*-acetylglucosamine (6'FN) (red diamonds), fucosyl-α-1,6-glucose (6'FucGlc) (pink triangles up), fucosyl-α-1,6-galactose (6'FucGal) (cyan crosses), fucosyl-α-1,6-*N*,*N*'-diacetylchitobiose (N2F *N*-glycan) (grey x) or *N*-acetylglucosamine (GlcNAc) (blue triangles down). The four mutant strains were grown in MRS basal medium with GlcNAc as a positive control. (E) HPLC chromatograms (Dionex system) of the supernatants (10 times diluted) from *Lactobacillus casei* strain cultures. Chromatograms of the standard L-fucose 0.4 mM (1), *N*-acetylglucosamine (GlcNAc)

0.1 mM (2), *N*-acetylglucosamine-asparagine (GlcNAc-Asn) 0.1 mM (3) and fucosyl-α-1,6-*N*-acetylglucosamine-asparagine (6'FN-Asn) 0.1 mM (4). Chromatograms of the culture supernatants from *L. casei* BL23 (WT) cultured without added sugar (5) or from *L. casei* strains cultured on 6'FN-Asn: BL23 (WT) (6), BL418 (*asnA2*) (7), BL417 (*pepV*) (8) BL416 (*asdA*) (9), BL415 (*alfC*) (10), BL372 (*alfH*) (11), BL392 (*sugK*) (12) and BL405 (*alfR2*) (13). The numbers by the L-fucose peaks indicated the concentration in mM.

Figure 6. Growth curves of *Lactobacillus casei* mutant strains. BL416 (*asdA*) (A), BL417 (*pepV*) (B), BL418 (*asnA2*) (C) and BL392 (*sugK*) (D) on MRS basal medium without carbon source (black squares), with fucosyl-α-1,6-*N*-acetylglucosamine-asparagine (6'FN-Asn) (green circles) or *N*-acetylglucosamine (GlcNAc) (blue triangles). In all graphs, the growth pattern of the wild-type (WT) strain BL23 is represented for a better comparison.

Figure 7. Structural organization of the *alf2* gene clusters from *Lactobacillus rhamnosus* GG, *Lactobacillus heilongjiangensis* DSM 28069, *Lactobacillus nantensis* DSM 16982, *Lactobacillus melliventris* Hma8, *Bifidobacterium asteroides* Bin2, *Bifidobacterium actinocoloniiforme* DSM 22766, *Lactobacillus manihotivorans* DSM 13343, *Lactobacillus gasseri* ATCC 33323, *Lactobacillus johnsonii* ATCC 33200, *Lactobacillus curvatus* MRS6, *Lactobacillus sakei* LS25. Stem-loop structures in *L. casei* DNA represent putative *rho*-independent terminators. Surrounding genes near the *alf2* genes are also shown. The organization of the *Lactobacillus casei* BL23 *alf2* operon is also shown for a better comparison.

SUPPLEMENTAL MATERIAL FILES

Table S1. ^{1}H and ^{13}C assignment of compounds fucosyl-α-1,6-*N*-acetylglucosamine-asparagine, fucosyl-α-1,6-*N*,*N*'-diacetylchitobiose, fucosyl-α-1,6-galactose and fucosyl-α-1,6-glucose carried out at 27 °C and 600 MHz in D_2O. The spectrum was referenced to the water signal at 4.7 ppm.

Table S2. Final O.D. values (means ± standard deviation) reached by *Lactobacillus casei* mutant strains cultured on 6'fucosyl glycans.

Table S3. Primers used in this study.

Fig. S1. Zoom of 2D HMBC NMR spectrum of compound fucosyl-α-1,6-*N*-acetylglucosamine-asparagine in D_2O acquired at 27 °C and 600 MHz with an inverse cryoprobe. The correlation between C 1' and H6a and H6b clearly reflects the binding 1,6 between both sugar molecules.

Fig. S2 (**A**) SDS-polyacrylamide gel (PAGE) analysis of the protein AsnA2. SDS-PAGE electrophoresis was performed in 12% gels under reducing conditions, and the proteins were Coomassie blue stained. Lane P, protein standards. The numbers on the left are molecular masses. The arrows on the right point the AsnA2 protein bands. (**B**) Chromatogram showing the size exclusion chromatography of AsnA2. All products elute as a single peak with an estimated molecular weight of 55.6 kDa. (**C**) Calibration plot of standard proteins. Gel filtration experiments with five standard proteins were used. (**D**) Deglycosylation assays: SDS-PAGE analysis of ovalbumin (OVA) and lactoferrin (LAC) wihouth (-) and with (+) glycosylasparaginase AsnA2. SDS-PAGE electrophoresis was performed in 10% gels under reducing conditions, and the proteins

were Coomassie blue stained. Lane P, protein standards. The numbers on the right are molecular masses. **(E)** HPLC chromatrograms (Dionex system) of reaction mixtures containing 0.2 μg of AsnA2 enzyme, 100 mM Tris-HCl buffer, pH 7.0 and 5 mM of GlcNAc-Asn (chromatograms 5, 6 and 7 correspond to 0.5, 2 and 4 min of reaction time, respectively) and 6'FN-Asn (chromatograms 8, 9 and 10 correspond to 0.5, 2 and 4 min of reaction time, respectively). Each reaction was diluted 20 times before HPLC analysis. The red arrows showed the GlcNAc released by AsnA2 from GlcNAc-Asn and the blue arrows showed the 6'FN released from 6'FN-Asn in the Figure in zoom. Chromatograms of the standards at 0.1 mM: *N*-acetylglucosamine (GlcNAc) (1), *N*-acetylglucosamine-asparagine (GlcNAc-Asn) (2); fucosyl-α-1,6-*N*-acetylglucosamine (6'FN) (3) and fucosyl-α-1,6-*N*-acetylglucosamine-asparagine (6'FN-Asn) (4).

Fig. S3. Maximum likelihood phylogenetic trees of AlfC (A) and AlfH (B) protein sequences. Sequence accession numbers are indicated in parentheses. Support values higher than 750 for the bootstrap analysis are indicated. The blue bracket indicates the cluster containing the corresponding *Lactobacillus casei* sequence.

Fig. S4. Maximum likelihood phylogenetic trees of AsnA2 protein sequences. Sequence accession numbers are indicated in parentheses. Support values higher than 750 for the bootstrap analysis are indicated. The blue bracket indicates the cluster containing the corresponding *Lactobacillus casei* sequence.

Fig. S5. Maximum likelihood phylogenetic trees of AsdA protein sequences. Sequence accession numbers are indicated in parentheses. Support values higher than 750 for the bootstrap analysis are indicated. The blue bracket indicates the cluster containing the corresponding *Lactobacillus casei* sequence.

Fig. S6. Maximum likelihood phylogenetic trees of PepV protein sequences. Sequence accession numbers are indicated in parentheses. Support values higher than 750 for the bootstrap analysis are indicated. The blue bracket indicates the cluster containing the corresponding *Lactobacillus casei* sequence.

Fig. 1

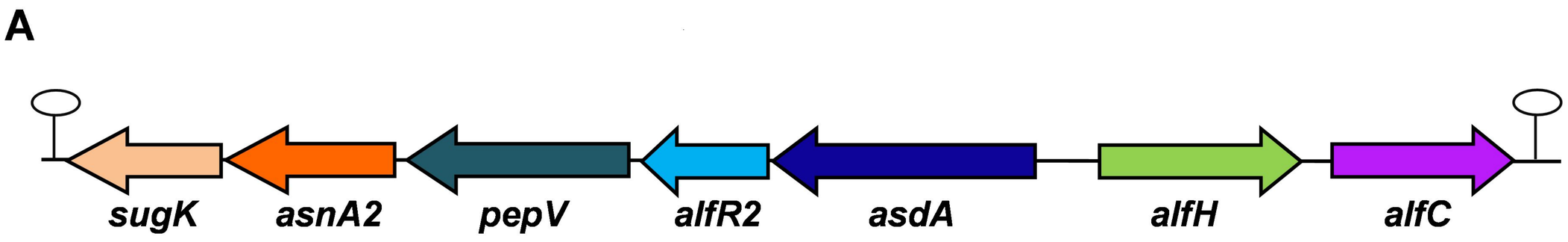
A
sugK
asnA2
pepV
alfR2
asdA
alfH
alfC

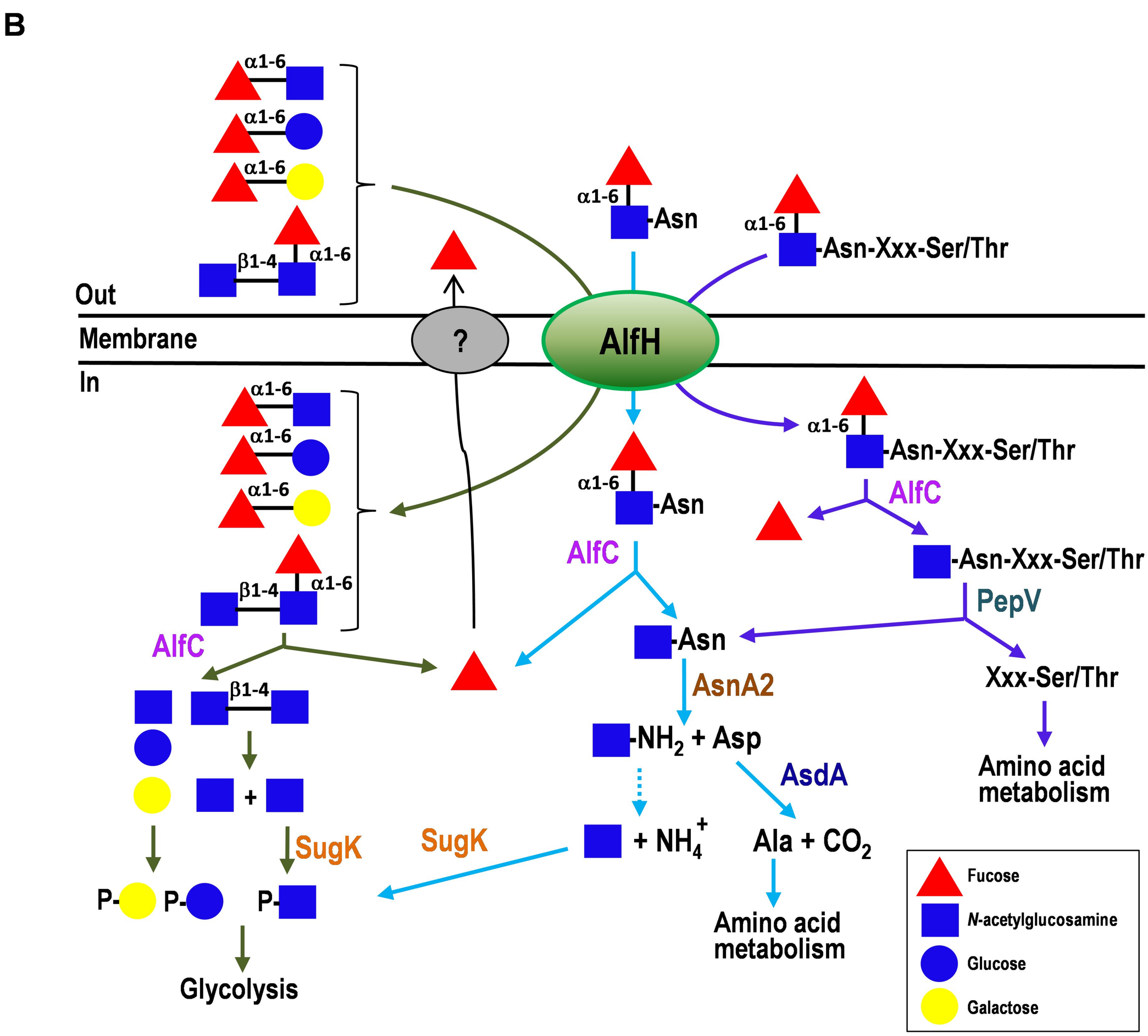
B
α1-6
β1-4
Out
Membrane
In
?
AlfH
-Asn
-Asn-Xxx-Ser/Thr
AlfC
PepV
AsnA2
AsdA
SugK
-NH2 + Asp
+ NH4+
Ala + CO2
Xxx-Ser/Thr
Amino acid metabolism
Glycolysis
P-
Fucose
N-acetylglucosamine
Glucose
Galactose

Fig. 2

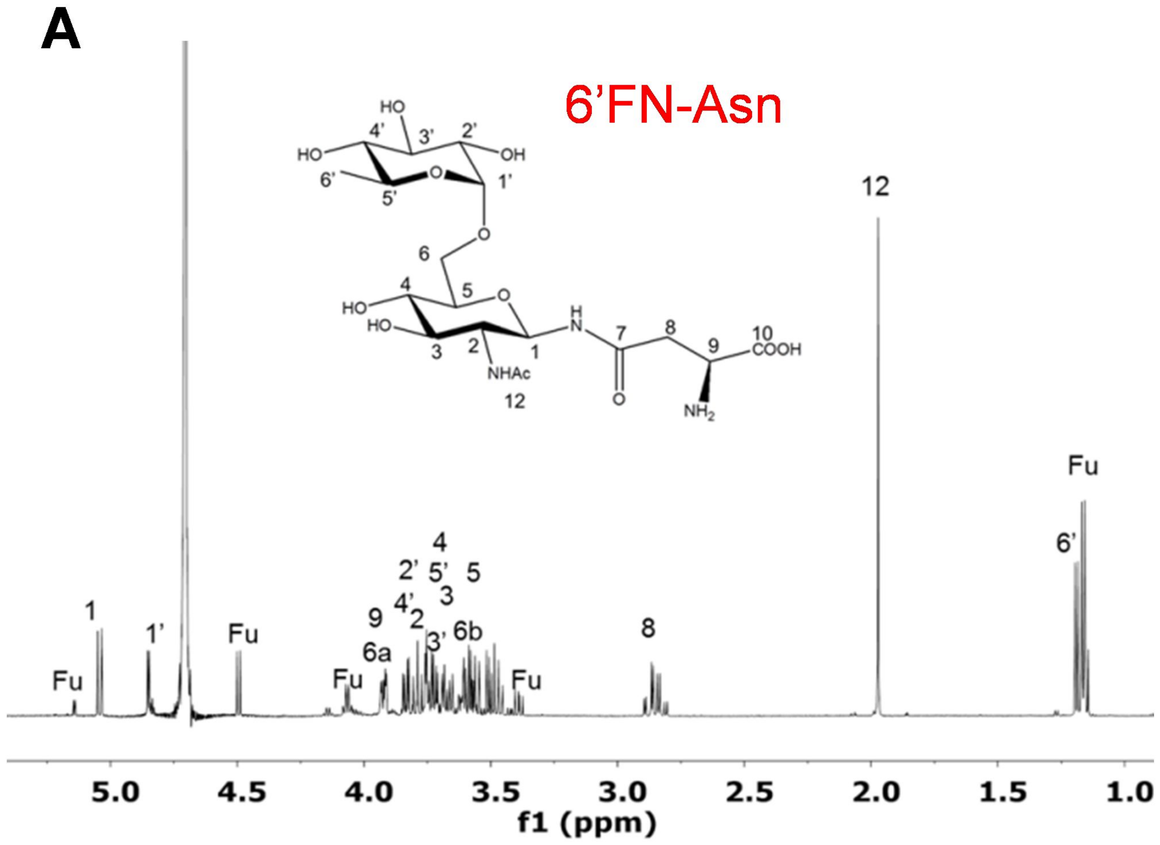
A
6'FN-Asn
12
Fu
6'
1
1'
Fu
Fu
Fu
Fu
9
6a
4
2' 5' 5
4' 2
3
3' 6b
8
5.0
4.5
4.0
3.5
3.0
2.5
2.0
1.5
1.0
f1 (ppm)

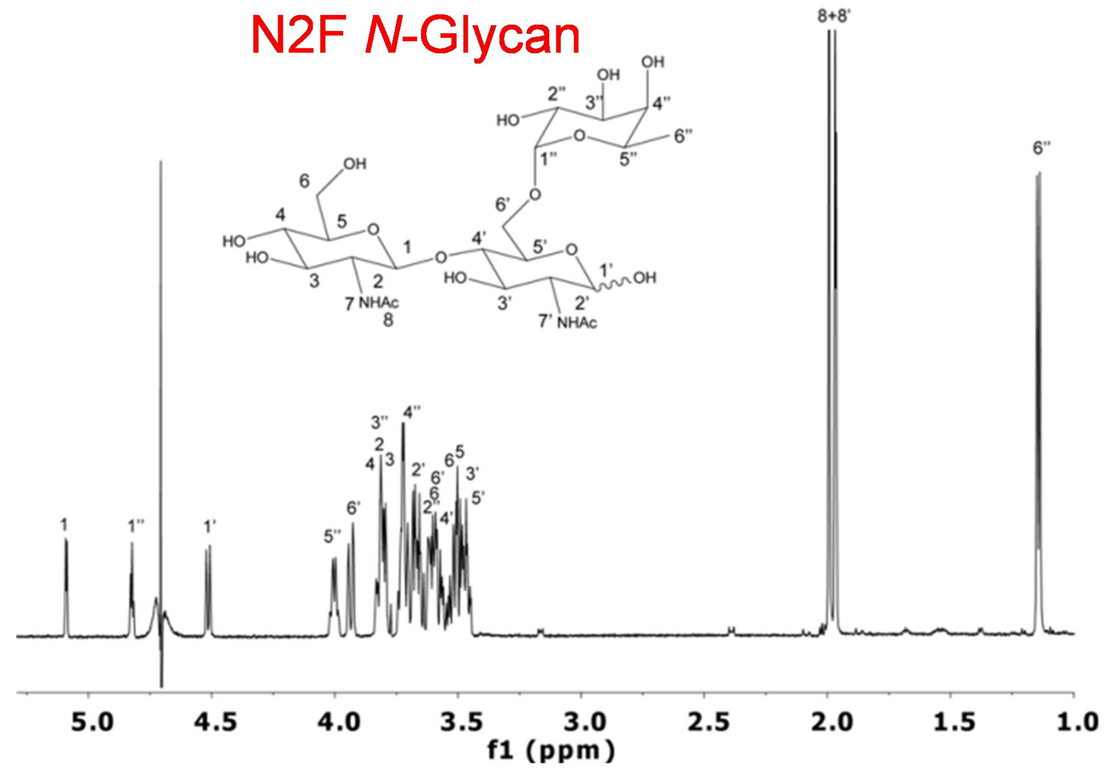
B
N2F N-Glycan
8+8'
6"
1
1"
1'
5"
6'
3"
4"
2
4
3
2'
6'
6
2"
4'
6
5
3'
5'
5.0
4.5
4.0
3.5
3.0
2.5
2.0
1.5
1.0
f1 (ppm)

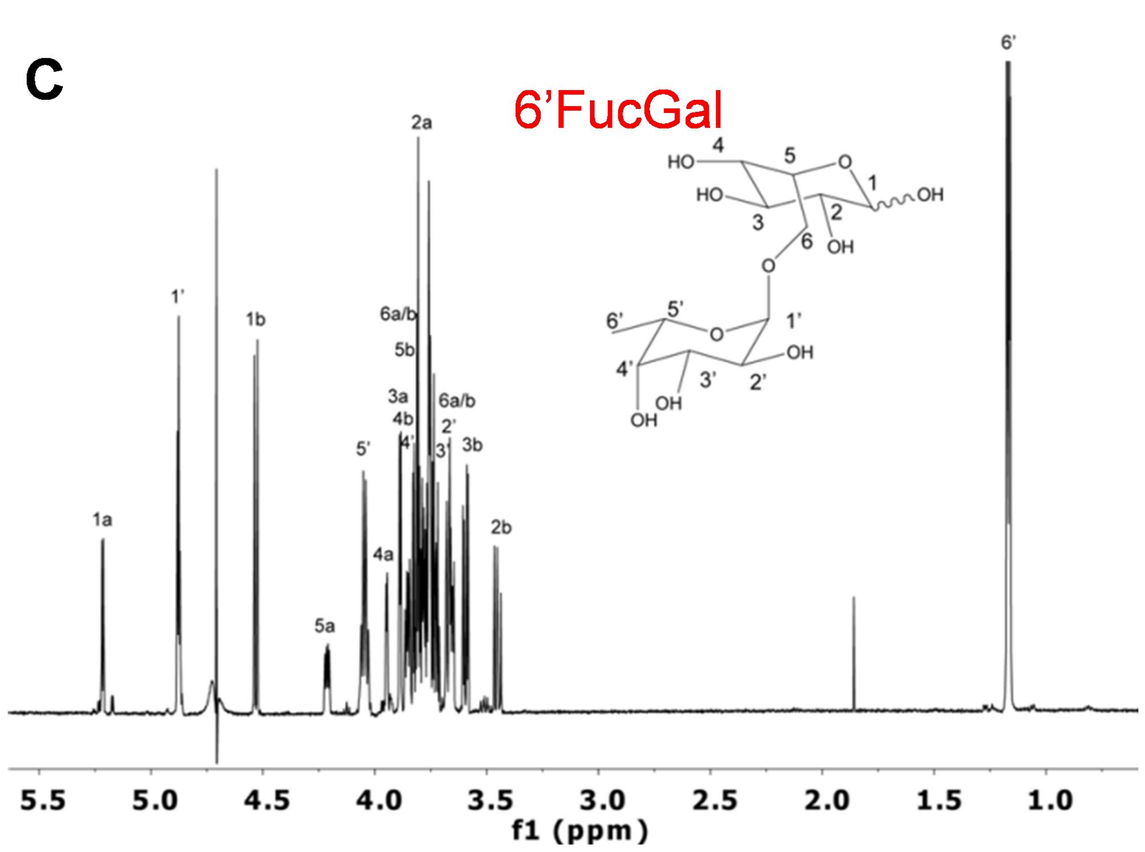
C
6'FucGal
6'
2a
1'
1b
6a/b
5b
3a
4b
6a/b
2'
5'
4'
3'
3b
1a
4a
2b
5a
5.5
5.0
4.5
4.0
3.5
3.0
2.5
2.0
1.5
1.0
f1 (ppm)

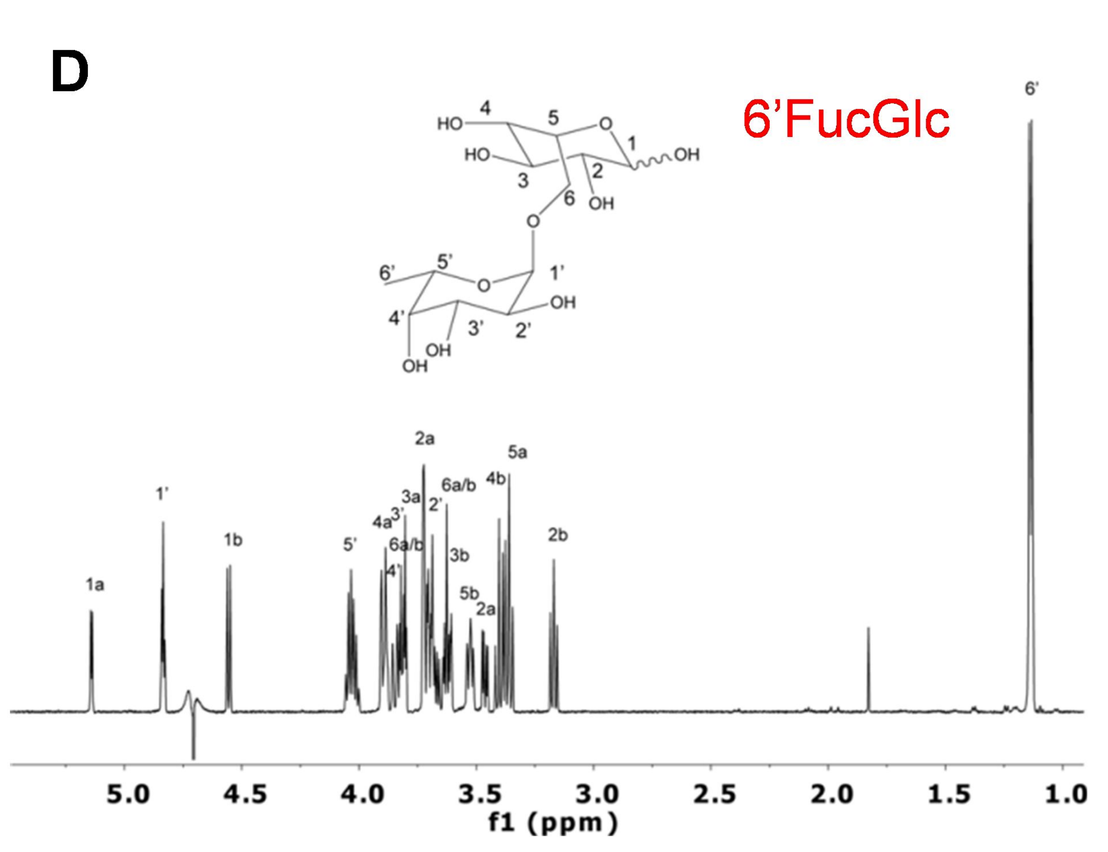
D
6'FucGlc
6'
2a
5a
1'
4b
6a/b
3a
4a
3'
2'
1b
5'
6a/b
3b
4'
2b
1a
5b
2a
5.0
4.5
4.0
3.5
3.0
2.5
2.0
1.5
1.0
f1 (ppm)

Fig. 3

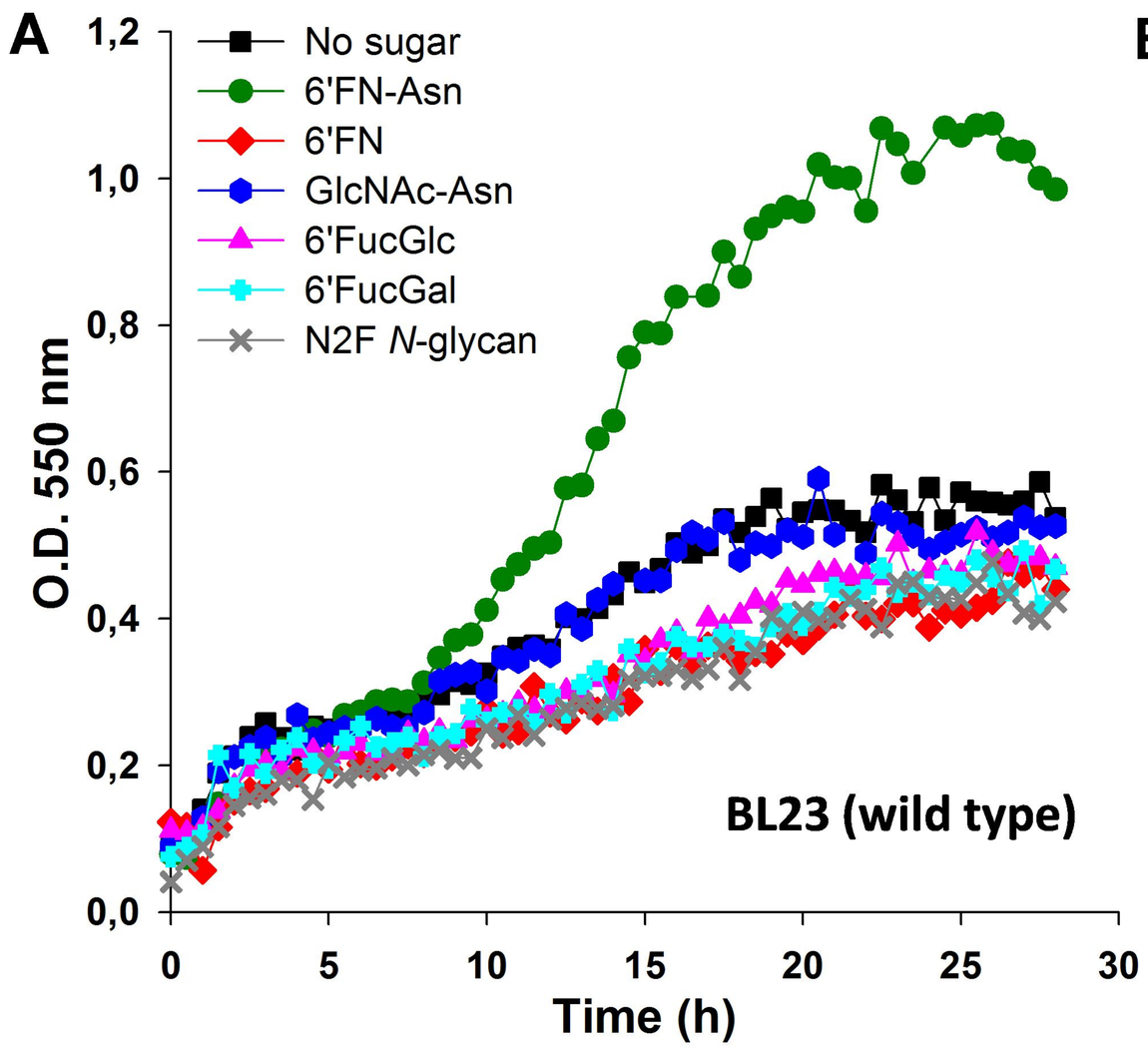
A
No sugar
6'FN-Asn
6'FN
GlcNAc-Asn
6'FucGlc
6'FucGal
N2F N-glycan
O.D. 550 nm
Time (h)
BL23 (wild type)

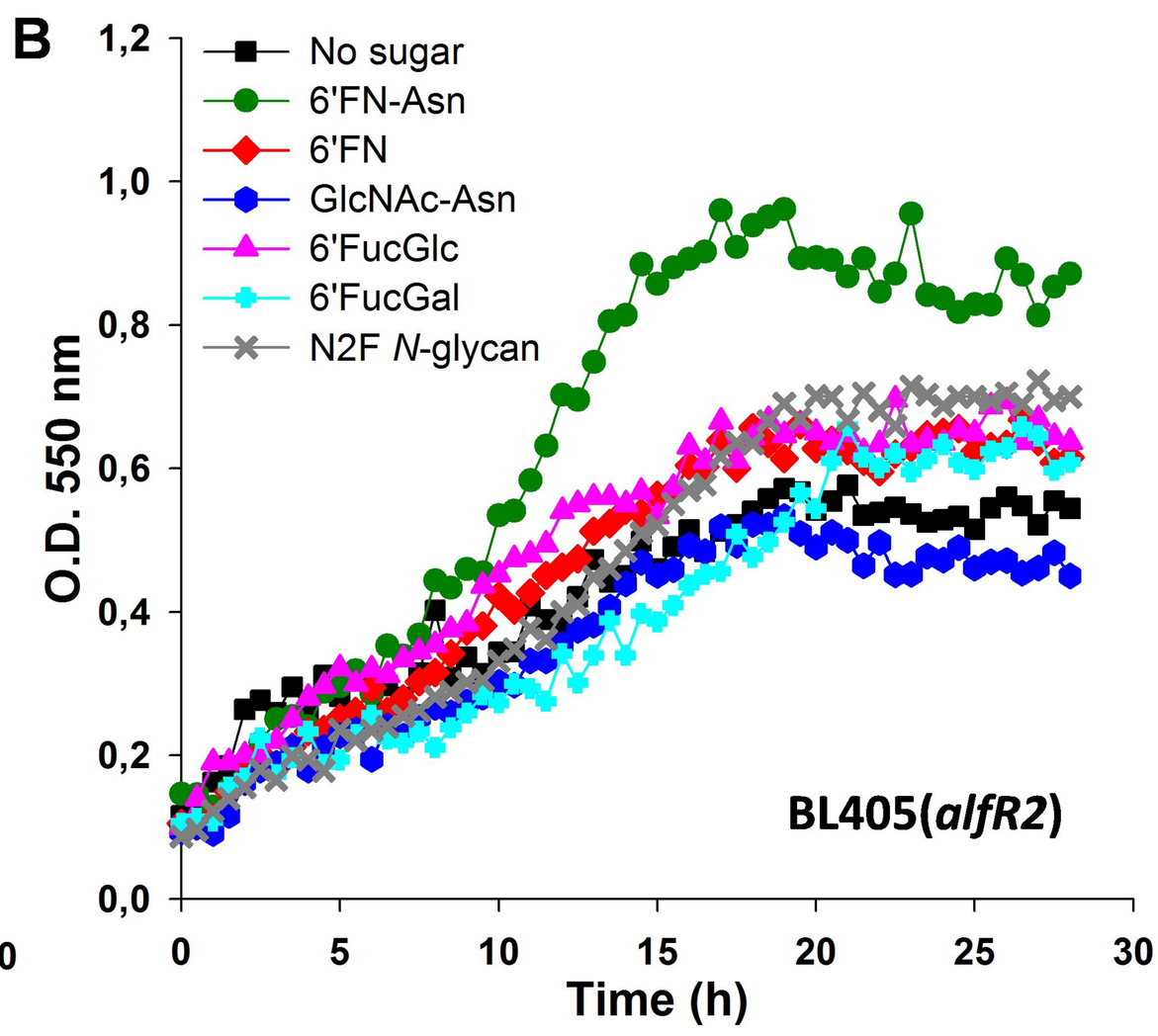
B
No sugar
6'FN-Asn
6'FN
GlcNAc-Asn
6'FucGlc
6'FucGal
N2F N-glycan
O.D. 550 nm
Time (h)
BL405(alfR2)

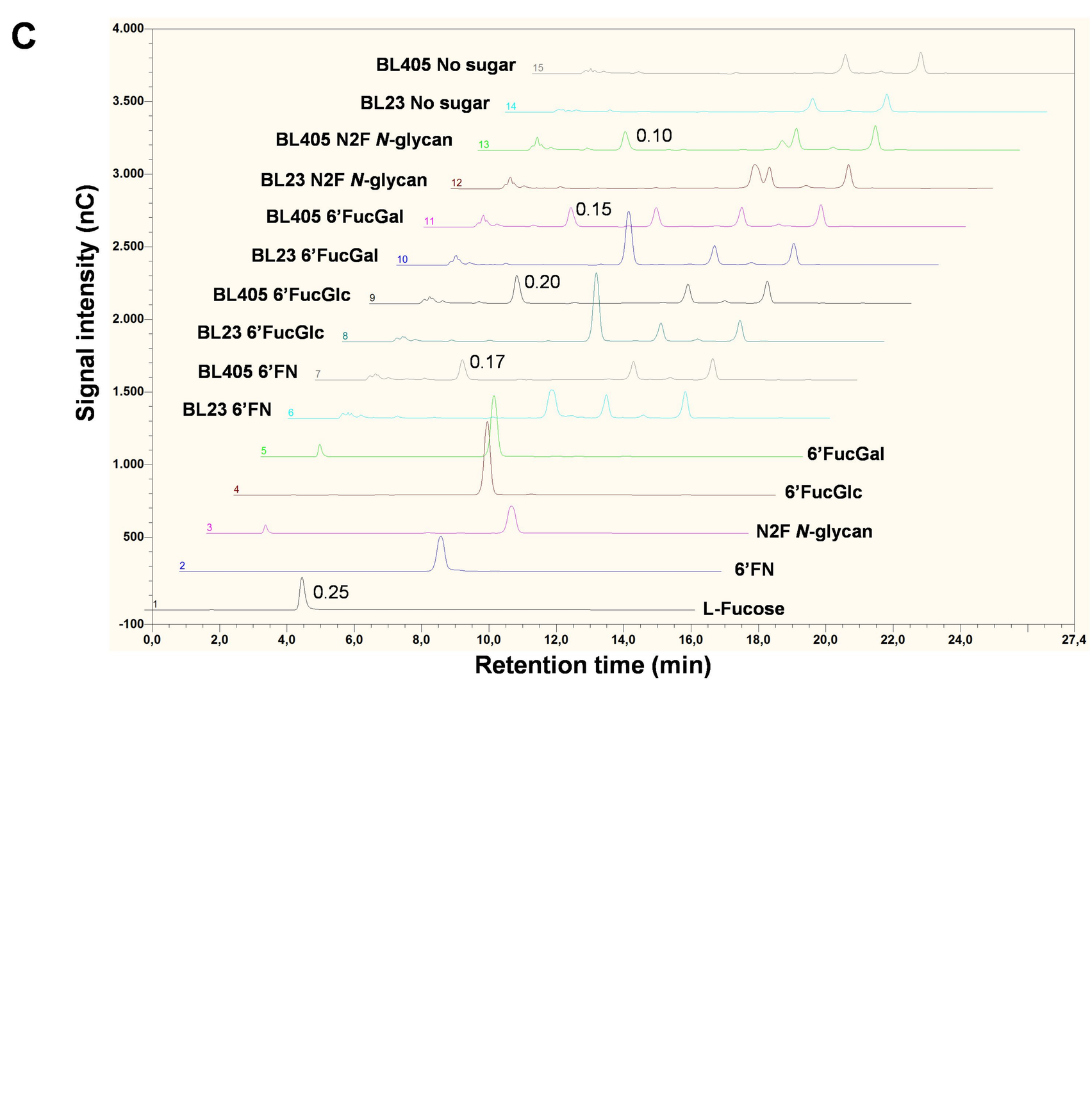
C
Signal intensity (nC)
BL405 No sugar
BL23 No sugar
BL405 N2F N-glycan
BL23 N2F N-glycan
BL405 6'FucGal
BL23 6'FucGal
BL405 6'FucGlc
BL23 6'FucGlc
BL405 6'FN
BL23 6'FN
6'FucGal
6'FucGlc
N2F N-glycan
6'FN
L-Fucose
0.10
0.15
0.20
0.17
0.25
Retention time (min)

Fig. 4

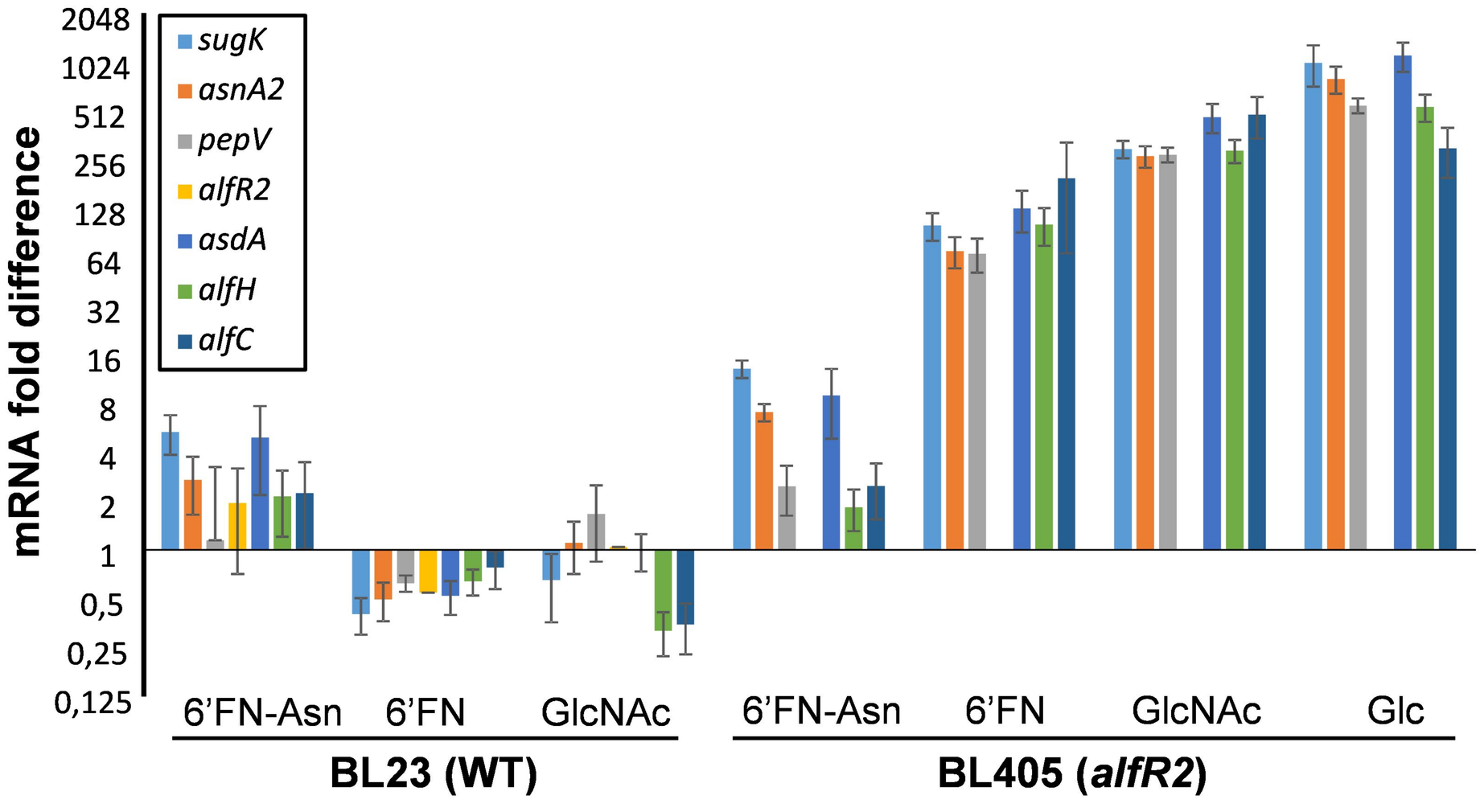
2048
1024
512
256
128
64
32
16
8
4
2
1
0,5
0,25
0,125
mRNA fold difference
sugK
asnA2
pepV
alfR2
asdA
alfH
alfC
6'FN-Asn
6'FN
GlcNAc
6'FN-Asn
6'FN
GlcNAc
Glc
BL23 (WT)
BL405 (alfR2)

Fig. 5

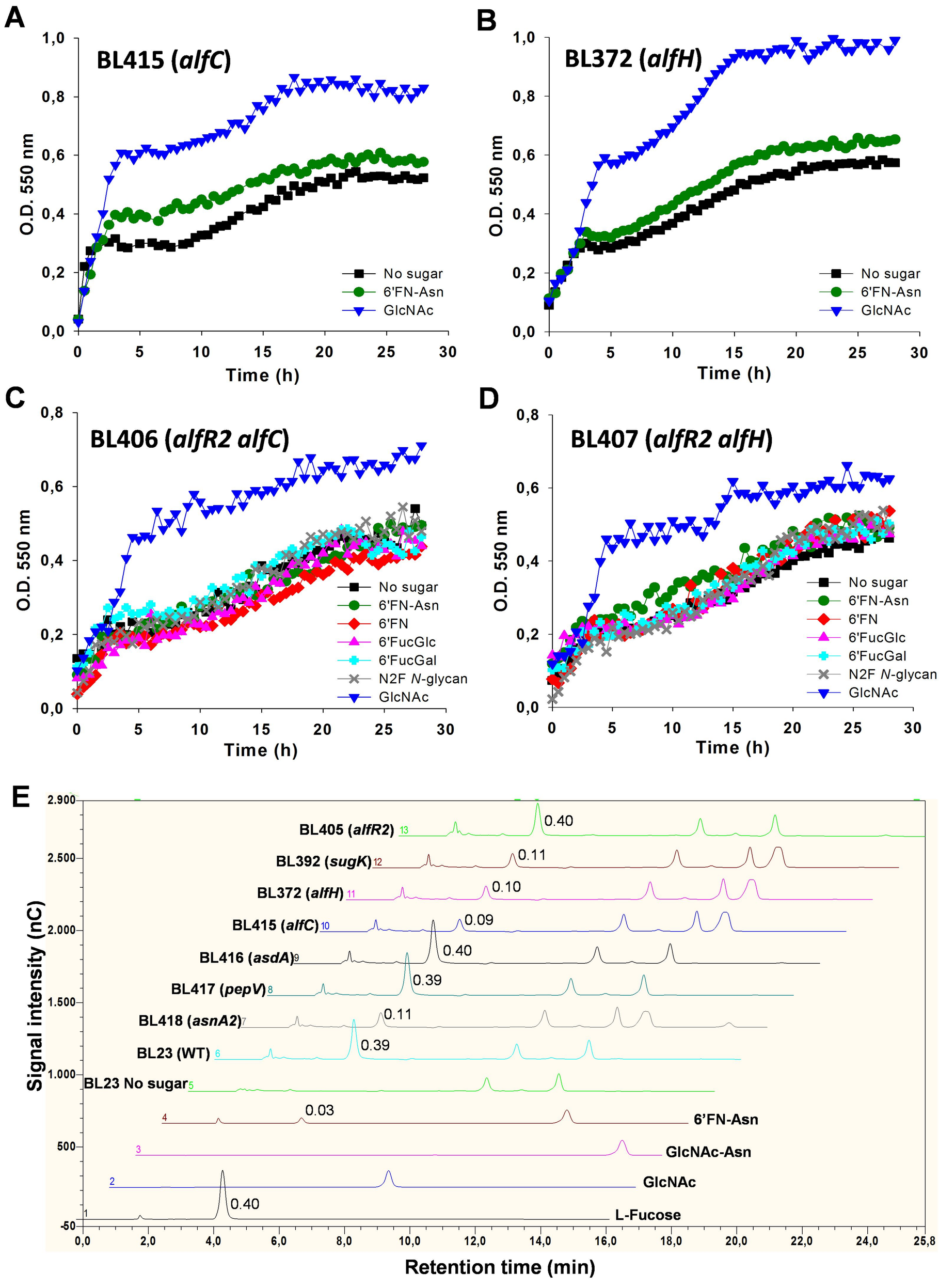
A
BL415 (alfC)
O.D. 550 nm
Time (h)
No sugar
6'FN-Asn
GlcNAc
B
BL372 (alfH)
C
BL406 (alfR2 alfC)
6'FN
6'FucGlc
6'FucGal
N2F N-glycan
D
BL407 (alfR2 alfH)
E
Signal intensity (nC)
Retention time (min)
BL405 (alfR2)
BL392 (sugK)
BL372 (alfH)
BL415 (alfC)
BL416 (asdA)
BL417 (pepV)
BL418 (asnA2)
BL23 (WT)
BL23 No sugar
6'FN-Asn
GlcNAc-Asn
GlcNAc
L-Fucose
0.40
0.11
0.10
0.09
0.39
0.03

Fig. 6

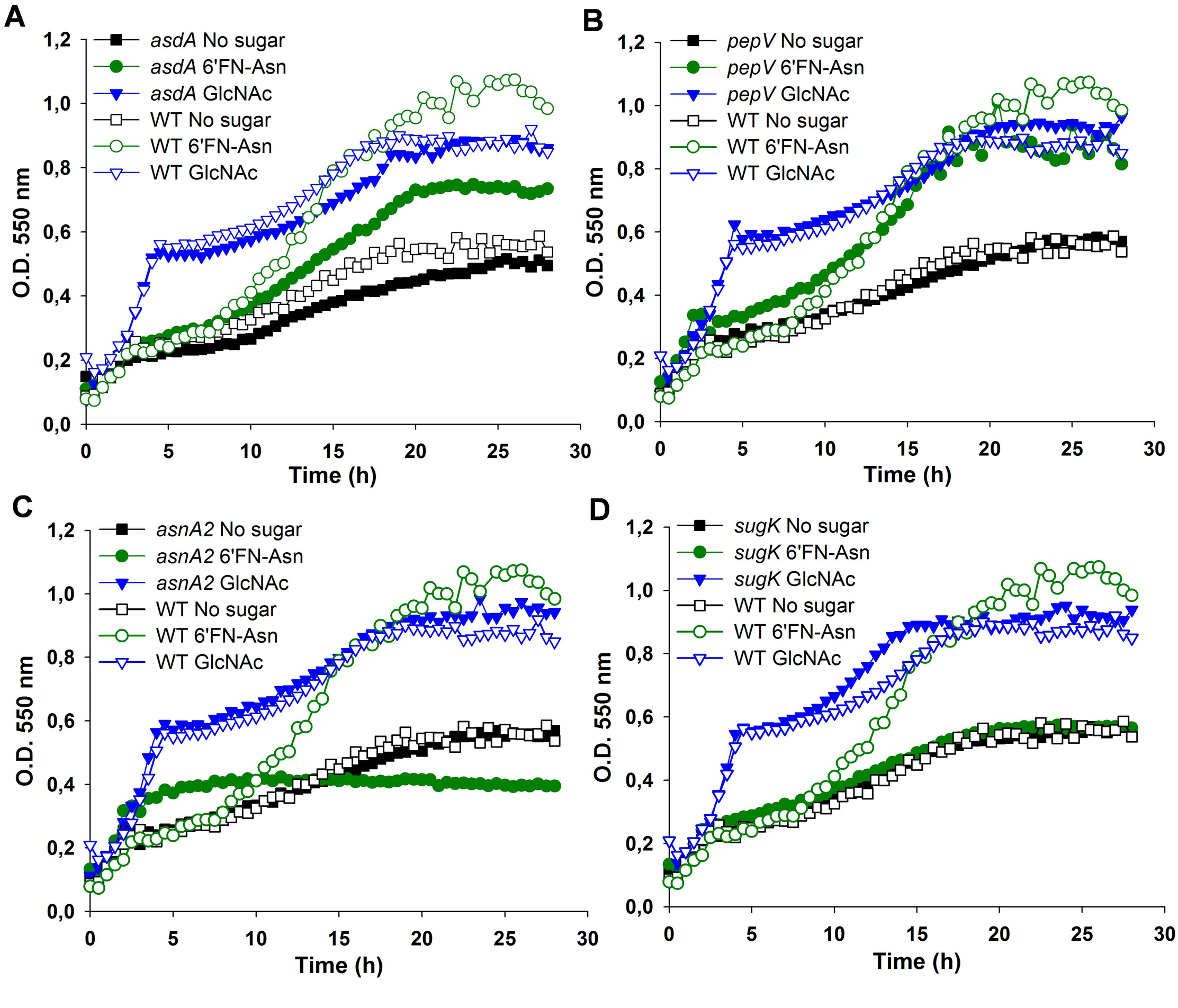
A
asdA No sugar
asdA 6'FN-Asn
asdA GlcNAc
WT No sugar
WT 6'FN-Asn
WT GlcNAc
O.D. 550 nm
Time (h)
B
pepV No sugar
pepV 6'FN-Asn
pepV GlcNAc
WT No sugar
WT 6'FN-Asn
WT GlcNAc
O.D. 550 nm
Time (h)
C
asnA2 No sugar
asnA2 6'FN-Asn
asnA2 GlcNAc
WT No sugar
WT 6'FN-Asn
WT GlcNAc
O.D. 550 nm
Time (h)
D
sugK No sugar
sugK 6'FN-Asn
sugK GlcNAc
WT No sugar
WT 6'FN-Asn
WT GlcNAc
O.D. 550 nm
Time (h)

Fig. 7

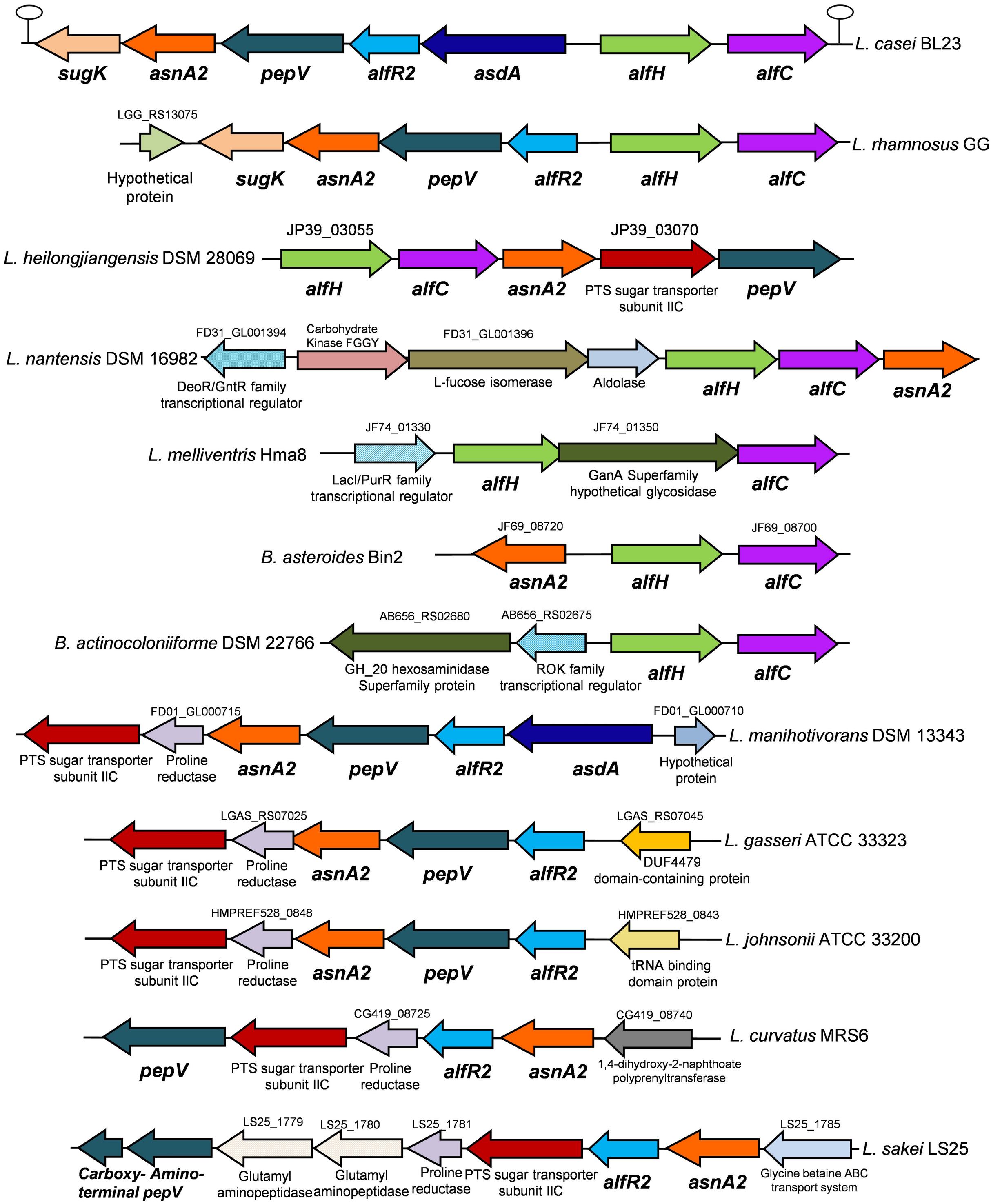
sugK
asnA2
pepV
alfR2
asdA
alfH
alfC
L. casei BL23
LGG_RS13075
Hypothetical protein
sugK
asnA2
pepV
alfR2
alfH
alfC
L. rhamnosus GG
JP39_03055
JP39_03070
L. heilongjiangensis DSM 28069
alfH
alfC
asnA2
PTS sugar transporter subunit IIC
pepV
FD31_GL001394
Carbohydrate Kinase FGGY
FD31_GL001396
L. nantensis DSM 16982
DeoR/GntR family transcriptional regulator
L-fucose isomerase
Aldolase
alfH
alfC
asnA2
JF74_01330
JF74_01350
L. melliventris Hma8
LacI/PurR family transcriptional regulator
alfH
GanA Superfamily hypothetical glycosidase
alfC
JF69_08720
JF69_08700
B. asteroides Bin2
asnA2
alfH
alfC
AB656_RS02680
AB656_RS02675
B. actinocoloniiforme DSM 22766
GH_20 hexosaminidase Superfamily protein
ROK family transcriptional regulator
alfH
alfC
FD01_GL000715
FD01_GL000710
L. manihotivorans DSM 13343
PTS sugar transporter subunit IIC
Proline reductase
asnA2
pepV
alfR2
asdA
Hypothetical protein
LGAS_RS07025
LGAS_RS07045
L. gasseri ATCC 33323
PTS sugar transporter subunit IIC
Proline reductase
asnA2
pepV
alfR2
DUF4479 domain-containing protein
HMPREF528_0848
HMPREF528_0843
L. johnsonii ATCC 33200
PTS sugar transporter subunit IIC
Proline reductase
asnA2
pepV
alfR2
tRNA binding domain protein
CG419_08725
CG419_08740
L. curvatus MRS6
pepV
PTS sugar transporter subunit IIC
Proline reductase
alfR2
asnA2
1,4-dihydroxy-2-naphthoate polyprenyltransferase
LS25_1779
LS25_1780
LS25_1781
LS25_1785
L. sakei LS25
Carboxy- Amino-terminal pepV
Glutamyl aminopeptidase
Glutamyl aminopeptidase
Proline reductase
PTS sugar transporter subunit IIC
alfR2
asnA2
Glycine betaine ABC transport system